

# Quantitative proteomics reveals metabolic and pathogenic properties of *Chlamydia trachomatis* developmental forms

Hector A. Saka,<sup>1</sup> J. Will Thompson,<sup>2</sup> Yi-Shan Chen,<sup>1</sup>  
Yadunanda Kumar,<sup>1†</sup> Laura G. Dubois,<sup>2</sup>  
M. Arthur Moseley<sup>2</sup> and Raphael H. Valdivia<sup>1\*</sup>

<sup>1</sup>Department of Molecular Genetics and Microbiology  
and Center for Microbial Pathogenesis and <sup>2</sup>Proteomics  
Core Facility, Duke University Medical Center, Durham,  
NC, USA.

## Summary

*Chlamydia trachomatis* is an obligate intracellular pathogen responsible for ocular and genital infections of significant public health importance. *C. trachomatis* undergoes a biphasic developmental cycle alternating between two distinct forms: the infectious elementary body (EB), and the replicative but non-infectious reticulate body (RB). The molecular basis for these developmental transitions and the metabolic properties of the EB and RB forms are poorly understood as these bacteria have traditionally been difficult to manipulate through classical genetic approaches. Using two-dimensional liquid chromatography – tandem mass spectrometry (LC/LC-MS/MS) we performed a large-scale, label-free quantitative proteomic analysis of *C. trachomatis* LGV-L2 EB and RB forms. Additionally, we carried out LC-MS/MS to analyse the membranes of the pathogen-containing vacuole ('inclusion'). We developed a label-free quantification approaches to measure protein abundance in a mixed-proteome background which we applied for EB and RB quantitative analysis. In this manner, we catalogued the relative distribution of > 54% of the predicted proteins in the *C. trachomatis* LGV-L2 proteome. Proteins required for central metabolism and glucose catabolism were predominant in the EB, whereas proteins associated with protein synthesis, ATP generation and nutrient transport were more abundant in the RB. These findings suggest that the EB is primed for a burst in metabolic activity upon entry, whereas the RB form is geared towards nutrient utilization, a rapid

increase in cellular mass, and securing the resources for an impending transition back to the EB form. The most revealing difference between the two forms was the relative deficiency of cytoplasmic factors required for efficient type III secretion (T3S) in the RB stage at 18 h post infection, suggesting a reduced T3S capacity or a low frequency of active T3S apparatus assembled on a 'per organism' basis. Our results show that EB and RB proteomes are streamlined to fulfil their predicted biological functions: maximum infectivity for EBs and replicative capacity for RBs.

## Introduction

The obligate intracellular bacterium *Chlamydia trachomatis* is an important human pathogen that causes a variety of ocular and genital infections of significant clinical and public health importance. *C. trachomatis* is the most common bacterial cause of sexually transmitted diseases (WHO, 2001; Miller *et al.*, 2004) and trachoma, the leading cause of infectious blindness worldwide (WHO, 2003; Burton and Mabey, 2009). A significant proportion of genital infections caused by *C. trachomatis* are left untreated due to their asymptomatic nature (Stamm, 1999), leading to serious complications including pelvic inflammatory disease, ectopic pregnancies and infertility, primarily in young women (Bebear and de Barbeyrac, 2009; Haggerty *et al.*, 2010). Additionally, neonates exposed to this bacterium in the birth process can develop complications in the first months of life such as conjunctivitis and/or pneumonia (Darville, 2005).

As all bacteria within the family *Chlamydiaceae*, *C. trachomatis* undergoes a unique, biphasic developmental cycle alternating between two forms with clear functional differences. The elementary body (EB) is environmentally stable, metabolically dormant, infectious and smaller in size compared with the reticulate body (RB), which is environmentally labile, highly replicative and non-infectious. Shortly after attachment, EBs secrete proteins into epithelial cells to promote their uptake (Clifton *et al.*, 2004; Dautry-Varsat *et al.*, 2005). Once inside the cell, the EB transitions to the RB form which replicates within a membrane-enclosed parasitophorous vacuole termed an 'inclusion'. As the inclusion expands, replication becomes asynchronous and RBs begin to differentiate

Accepted 8 October, 2011. \*For correspondence. E-mail valdi001@mc.duke.edu; Tel. (+1) 919 668 3831; Fax (+1) 919 681 9193. †Present address: Singapore-MIT Alliance for Research & Technology (SMART)-Center ID-IRG #05-06M, CELs Bldg, 28 Medical Drive, Singapore-117456.

back into EBs. This differentiation involves a transition form, the intermediate body (IB), which can be observed under the electron microscope as an RB with a condensed nucleoid (Phillips *et al.*, 1984). Throughout the infectious cycle, the bacterium exports an arsenal of effector proteins both to the inclusion membrane and to the host cytosol in order to manipulate host processes (Betts *et al.*, 2009 and references therein). Notably, *Chlamydia* successfully avoids lysosomal fusion with the inclusion while selective interactions with other cellular compartments are maintained to grant the bacteria access to essential nutrients and allow intracellular survival (Valdivia, 2008; Saka and Valdivia, 2010 and references therein). At the end of the cycle, the inclusion occupies most of the host cell cytoplasm and EBs are released to the extracellular environment where other cells can be targeted for infection (Hybiske and Stephens, 2007). The transition from EB to RB, and back, all constitute obligatory steps in replication and dissemination of *Chlamydiae* and are likely achieved by functional partitioning of distinct sets of bacterial proteins into these developmental forms.

In the past decade, the genomes of numerous *Chlamydia* species and strains have been sequenced, providing a wealth of information as to the basic biology of these organisms (Stephens *et al.*, 1998; Read *et al.*, 2000; 2003; Thomson *et al.*, 2008). Also, transcriptional profiling of *Chlamydia* at various stages during the infectious cycle or during stress-induced persistence has provided a basic blueprint as to when each gene is activated (Belland *et al.*, 2003; Albrecht *et al.*, 2010). However, lack of information on when proteins are expressed and how their abundance changes during developmental transitions has limited our understanding of the physiology and pathogenesis of these experimentally fastidious organisms. Mass spectrometry (MS)-based methods for peptide identification and sequencing techniques allow the assessment of large-scale surveys of the repertoire of proteins expressed by an organism ('proteomics') and have been applied for the study of microbial pathogenesis (Bhavsar *et al.*, 2010). Indeed, several proteomics studies for *Chlamydia* have been published (Vandahl *et al.*, 2001; 2002a; Shaw *et al.*, 2002; Mukhopadhyay *et al.*, 2004; Wehrli *et al.*, 2004; Skipp *et al.*, 2005; Liu *et al.*, 2010), although they primarily relied on protein identification. Recent developments in MS coupled with powerful database search algorithms enable reliable and highly reproducible identification and quantification of up to thousands of proteins in highly complex mixtures (Nilsson *et al.*, 2010; Walther and Mann, 2010). Therefore, quantitative proteomics offers a unique opportunity to address the biology of genetically intractable pathogens like *C. trachomatis*.



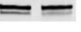

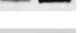
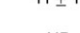





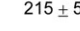

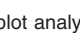
However, quantitative proteomic analyses on obligate intracellular pathogens like *Chlamydia* faces the unique challenge that isolation of pure bacterial protein extracts

without host protein contaminants is nearly impossible, which can introduce a significant quantitative bias especially when the contribution of host proteins to the total sample vary among developmental forms and experimental samples. To overcome this, we developed an extension of the 'absolute quantification' approach of Silva and Geromanos (Silva *et al.*, 2006a,b; Geromanos *et al.*, 2009). We applied this experimental approach to perform a detailed proteomic comparison of EB and RB forms by two-dimensional liquid chromatography – tandem mass spectrometry (LC/LC-MS/MS) (with both data-dependent and data-independent acquisition modes) (Delahunty and Yates, 2005; Silva *et al.*, 2006b). Additionally, we determined the compendium of chlamydial proteins associated to inclusion membranes by LC-MS/MS. Results from this study underscore how the differential composition of EB and RB proteomes reflects the adaptation of these two developmental forms to fulfil their main biological functions, which are to achieve maximum infectivity for EBs and replicative capacity for RBs.

## Results and discussion

### *Proteomic analysis of C. trachomatis developmental forms by LC/LC-MS/MS*

We chose a plaque purified *C. trachomatis*, biovar LGV, serovar L2, 434/Bu isolate for large-scale preparations and proteomic analysis. The developmental cycle of L2 434/Bu has been extensively characterized (Fig. S1A) (Nicholson *et al.*, 2003). Within 2–6 h post internalization, the EB differentiates into the RB form within nascent inclusions. Over the following hours, the RB increases in size and divides by binary fission, reaching maximum RB to EB ratio about 18–24 h post infection (hpi). At this stage, chlamydial replication becomes asynchronous and RBs initiate their differentiation back to the EB form with maximal production of infectious progeny and cell lysis occurring about 44–48 hpi (Nicholson *et al.*, 2003). For *C. trachomatis* L2, 18 hpi is the point of the cycle when the inclusion consists mostly of RBs with very few EBs, and some RB forms beginning their developmental transition back to the EB (Nicholson *et al.*, 2003). Earlier time points (i.e. 6 or 12 hpi) did not yield enough material for LC/LC-MS/MS and later time points (i.e. 30 or 36 hpi) would require the efficient separation of EBs and RBs at different stages of differentiation, which is currently not technically feasible. Therefore, to achieve maximal yields of each developmental form with minimal cross-contamination we purified RBs at 18 hpi and EBs at 44 hpi by sequential density gradients (Fig. S1B). A potential caveat to this approach is that the RB fraction we analysed represents a single time point during infection and its protein composition may not necessarily reflect that of RBs existing at earlier or later stages in the infectious cycle.

	Immunoblot		MS (fmol/ $\mu$ g)		Enrichment	
	EB	RB	EB	RB	Immunoblot	Proteomics
RpoD			70 $\pm$ 1	65 $\pm$ 9	no change	no change
RpoB			128 $\pm$ 4*	200 $\pm$ 38*	no change	no change
PmpD			11 $\pm$ 1	369 $\pm$ 45	RB	RB
IncG			ND	68 $\pm$ 15	RB	RB
CT288			67 $\pm$ 2	ND	EB	EB
Hc1			30 $\pm$ 5	ND	EB	EB
OmcB			215 $\pm$ 5*	47 $\pm$ 19*	EB	EB

**Fig. 1.** Immunoblot analysis of selected developmental stage-specific *C. trachomatis* proteins. The relative abundance in EBs and RBs for a subset of chlamydial proteins was determined by immunoblot analysis and compared with mass spectrometry (MS)-based quantification. Quantitative trends were defined as 'enrichment in EB' or 'enrichment in RB' when EB to RB fold change was  $\geq 2$  and  $\leq -2$ ; otherwise they were considered as 'no change'. Proteins that were below MS detection limits are indicated with 'ND' (not detected). Asterisks added to RpoB and OmcB quantitative values represent a 'quantitative flag', indicating that mass spectrometry-based quantification may be less accurate due to differences in the tryptic peptide profiles observed for those proteins.

Gradient purified bacteria were analysed by fluorescence microscopy and the EB fraction primarily showed small particles less than 0.5  $\mu$ m in size, compared with the RB-rich fraction, which showed larger ( $\sim 1$   $\mu$ m) cocci-shaped bacteria (Fig. S1C). The purified fractions were used to prepare total EB and RB protein lysates (Fig. S1D) and subjected to immunoblot analysis. Consistent with previous reports, the histone-like protein Hc1 which binds to the EB nucleoid (Wagar and Stephens, 1988) and the large cysteine-rich periplasmic protein OmcB (Watson *et al.*, 1994), were highly enriched in EB fractions whereas the early inclusion membrane protein IncG (Scidmore-Carlson *et al.*, 1999) was only detected in the RB form (Fig. 1). EB and RB total protein lysates were then digested with trypsin and the resulting peptides subjected to reverse phase LC/LC-MS/MS, allowing for the implementation of label-free, MS-based determination of protein abundance as previously described (Delahunty and Yates, 2005; Silva *et al.*, 2006b).

Despite extensive density gradient-based purification of bacteria, a total of 4360 unique peptides of human origin were detected, representing HeLa proteins that co-purified in our gradients. These 'mixed-species' proteomes challenge label-free quantification methods, especially when the relative contribution of each species to the resulting proteome varies significantly among samples that are to be compared directly (e.g. RB versus EB). To measure protein abundance in complex peptide mixtures containing a single target species and one or more 'contaminating' species, we modified a previously described 'absolute quantification' approach (Silva *et al.*,

2006b), so that even high levels of interference from other proteomes can be normalized out of the final quantitative measurement. Briefly, the methodology consisted of first calculating the fmol  $\mu$ g<sup>-1</sup> of each protein followed by normalization to the proteome of interest ('species-specific' correction). We validated this approach by analysing one sample representing a 'mixed proteome' (Sample 1, *Escherichia coli* and mouse brain lysates, 50% each) and another representing a 'pure proteome' (Sample 2, *E. coli* lysate). These samples were spiked with four selected proteins at pre-defined amounts and ratios prior to performing LC-MS/MS analysis and label-free quantification (Fig. 2A). There was a systematic bias in the *E. coli* and spiked-in proteins, which was corrected upon applying the experimentally derived 'species-specific' correction factor (Fig. 2B and C). Having accounted for these biases on quantification protocols, we proceeded to carry out the MS analysis of *C. trachomatis* EB and RB samples with differing degrees of human protein contamination. In addition, to directly compare EB and RB, samples were normalized on a 'per organism' basis, as detailed in *Experimental procedures*.

#### The *C. trachomatis* proteome

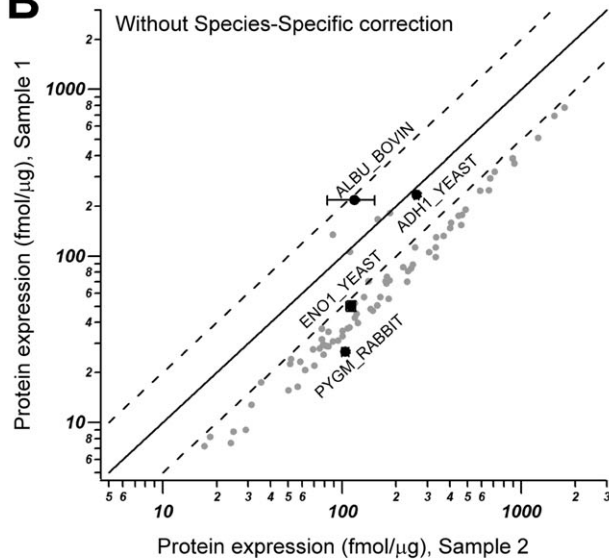
The MS analysis of *C. trachomatis* resulted in the identification of 4516 unique chlamydial peptides mapping to 485 non-redundant chlamydial proteins distributed between the two developmental forms and representing about 54% of the predicted proteome (Fig. 3A). The majority of identifications relied on multiple peptides per protein with 67.3% and 80.6% of proteins having two or more peptides detected in RB and EB forms respectively (Fig. 3B). The maximum number of unique peptides for the most abundant protein was > 100 (Table S1) and the average number of peptides per protein was  $\sim 9$  for EBs and  $\sim 5$  for RBs (data not shown). This is in contrast with a previous report where  $\sim 320$  chlamydial proteins were identified in EBs and RBs combined but  $\sim 52\%$  of them with only one peptide to match (Skipp *et al.*, 2005). The identification of multiple peptides per protein allowed the quantification of 373 non-redundant chlamydial proteins (Fig. 3A) with 97.6% of the proteins quantified with a relative standard deviation of less than 50% (Table S1 and data not shown).

We independently verified the MS-based quantification performed by immunoblot analysis of selected proteins. For example, CT288 a putative inclusion membrane protein (Inc) of unknown function, was determined by MS to be exclusively in EBs (Fig. 1). We generated antibodies against CT288 and confirmed that, like Hc1, this protein was mainly present in the EB, suggesting that this putative Inc protein, unlike other Inc proteins that are expressed during the RB stage (Giles *et al.*, 2006), per-

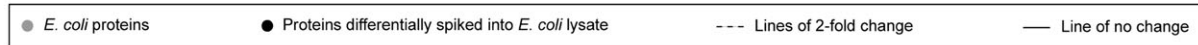
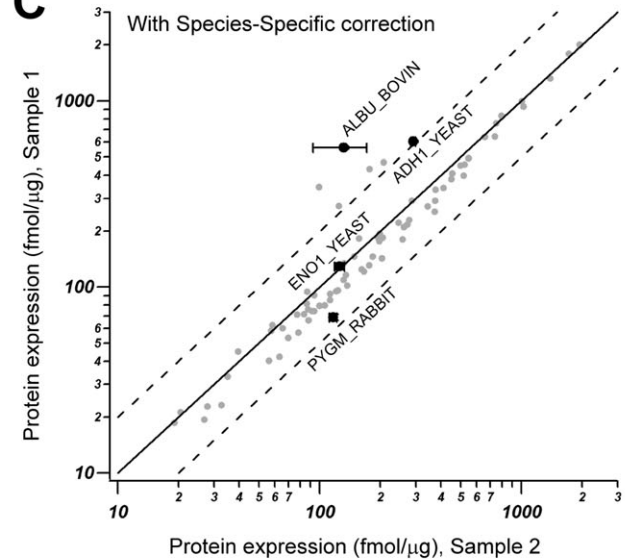
A

Protein Name	Quantification (fmol/ $\mu$ g)				Ratios		
	Sample 1 (uncorrected)	Sample 2 (uncorrected)	Sample 1 (corrected)	Sample 2 (corrected)	Measured Ratio (uncorrected)	Measured Ratio (corrected)	Theoretical Ratio
ALBU_BOVIN	217 $\pm$ 4	118 $\pm$ 35	561 $\pm$ 9	132 $\pm$ 39	1.80	4.30	4.00
ADH1_YEAST	234 $\pm$ 6	260 $\pm$ 7	604 $\pm$ 7	291 $\pm$ 7	0.90	2.10	2.00
ENO1_YEAST	50 $\pm$ 3	112 $\pm$ 7	129 $\pm$ 5	125 $\pm$ 7	0.50	1.00	2.00
PYGM_RABBIT	27.7 $\pm$ 0.5	105 $\pm$ 5	69 $\pm$ 3	117 $\pm$ 5	0.26	0.60	0.50
<i>E. coli</i> proteins (average)	109 $\pm$ 6	263 $\pm$ 17	281 $\pm$ 12	294 $\pm$ 19	0.41	0.96	1.00

B



C



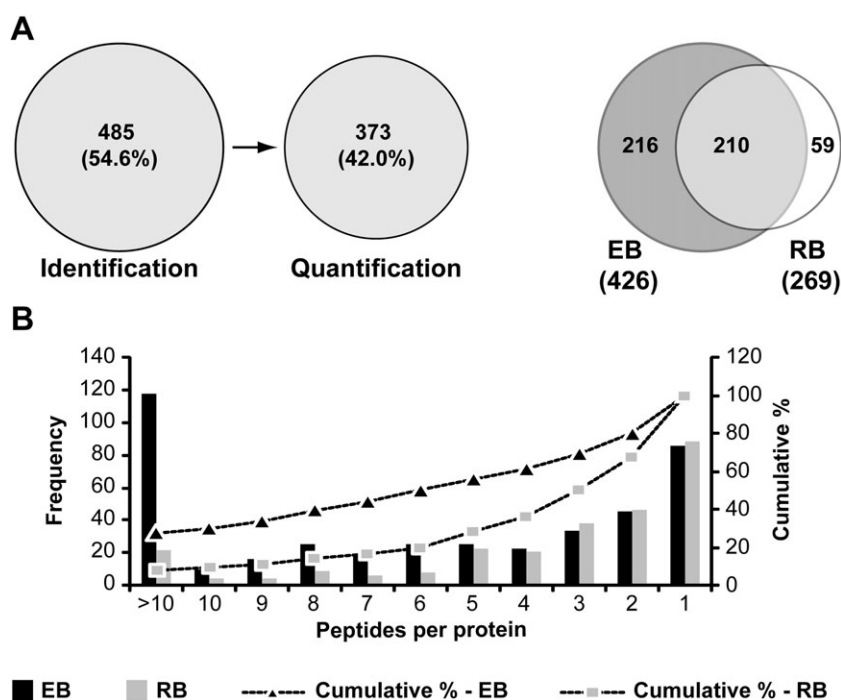
**Fig. 2.** Validation of label-free protein quantification of a complex mixture of proteins from two different species ('mixed proteomes').

A. We generated an artificial *E. coli*-mouse brain model system to assess the accuracy of MS-based label free quantification of proteins in a multi-species protein lysate. In addition, four exogenous proteins were spiked at pre-defined ratios as indicated (theoretical ratio) into 1:1 *E. coli*:mouse brain lysate (Sample 1, representing a 'mixed proteome') or *E. coli* lysates (Sample 2, representing a single proteome). After trypsin digestion and LC-MS/MS analysis, the quantitative measurements (fmol  $\mu$ g<sup>-1</sup>) of proteins were assessed with and without species-specific correction. When species-specific correction was applied, the corrected measured ratio was almost identical to the theoretical ratio. B and C. Lower panels show a graphic representation of the direct quantitative comparison of all proteins from Sample 1 and Sample 2, without and with species-specific correction, as indicated. Note that when all proteins in the sample are considered and no correction is applied (B), an obvious quantitative bias towards lower quantities in Sample 1 by approximately 2 $\times$  is observed, as expected. When using the total micrograms of only the identified *E. coli* proteins to normalize protein concentration as means of 'species-specific' correction (C), the result is that the correct ratio of *E. coli* and spiked-in proteins are reproduced. ADH1\_YEAST, yeast alcohol dehydrogenase; ENO1\_YEAST, yeast enolase; ALBU\_BOVIN, bovine albumin; PYGM\_RABBIT, rabbit glycogen phosphorylase. A logarithmic scale was used for x- and y-axis.

forms a function early upon EB invasion. Similarly, quantitative MS determined a higher abundance of PmpD in the RB form, which was also verified by immunoblots (Fig. 1). Other 'house-keeping' proteins, such as the core components of RNA polymerase, RpoD and RpoB, were present in equal amounts in the two developmental forms. Overall, we found a very good agreement between MS-based quantification and immunoblot analysis. However, a small subset (4%) of proteins identified displayed significant differences in the relative abundance of individual tryptic peptides generated between the EB and

RB forms. Consequently, for this subset of proteins the top three most abundant peptides were not entirely overlapped between EB and RB. Because the protein quantification algorithms used rely on a similar tryptic peptide profile being generated under the two experimental conditions, the comparative MS-based analysis for this protein subset may be less accurate. These proteins have been 'flagged' in our data sets (Table S1).

We annotated all proteins identified by MS, placed them in functional categories (Table S1), and determined the quantitative contribution of each category to the total EB



**Fig. 3.** Identification and quantification of the *C. trachomatis* L2 proteome.

A. Venn diagrams indicating the number of proteins identified and quantified by LC/LC-MS/MS (left panel) and the overlap in protein identification among the two *C. trachomatis* developmental forms (right panel).

B. Frequency histogram displays the distribution of the number of unique peptides per protein. The primary *y*-axis (bars) shows the number of proteins detected for each particular number of peptides per protein in EB and RB samples. The secondary *y*-axis (dotted lines) is a representation of the cumulative percentage of proteins detected along decreasing number of unique peptides per protein; 67.3% and 80.6% of proteins in EBs and RBs, respectively, were identified with two or more peptides to match.

and RB proteomes (Table 1). Notably, the six more prominent categories accounted for 76.4% and 80.5% of the total of EB and RB quantified proteins respectively (data not shown) and five out of these six top categories were shared between the two developmental forms (Table 1). However, their relative contribution to the total mass of EBs and RBs differed, particularly in the 'Translation', 'Energy Metabolism', 'Transport', 'Protein Folding' and 'Virulence & T3S' categories. Below we discuss how this

detailed MS-based analysis of the chlamydial proteome revealed new insights into *Chlamydia* biology.

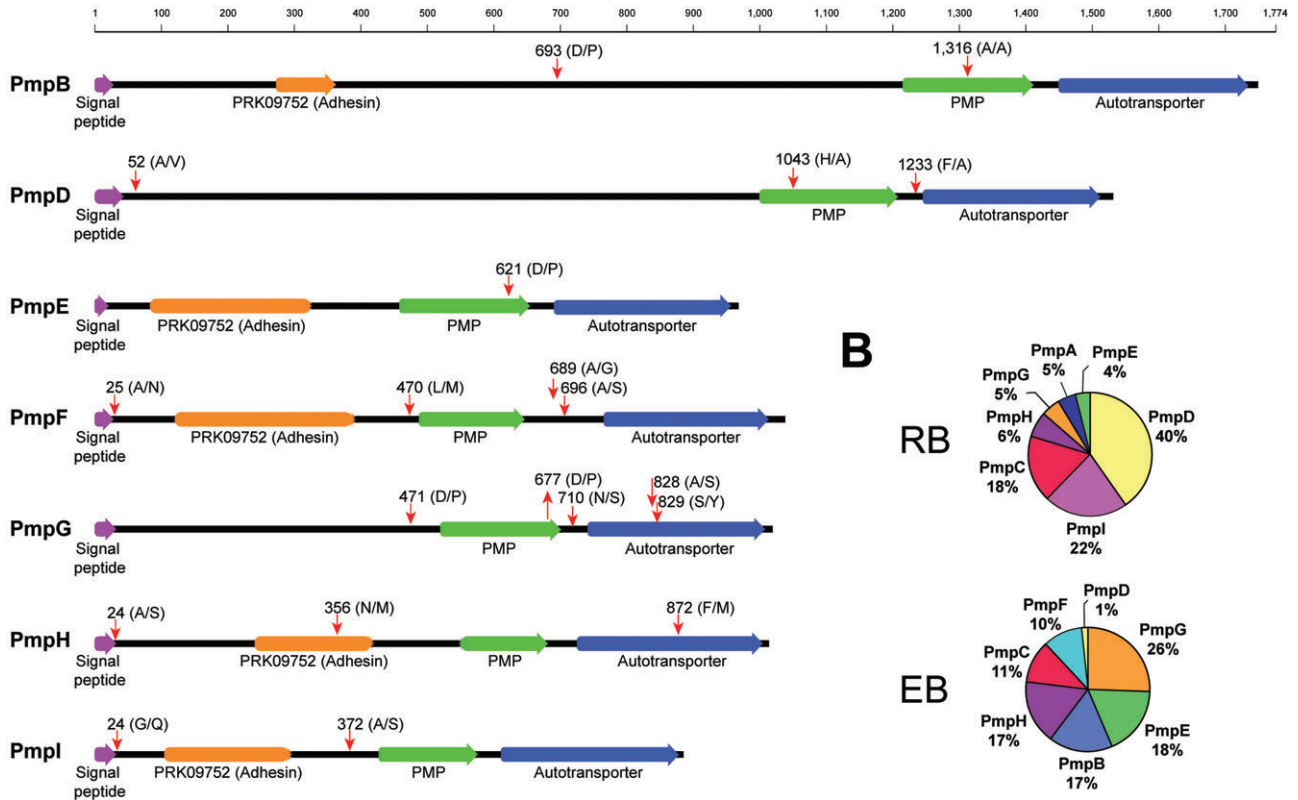
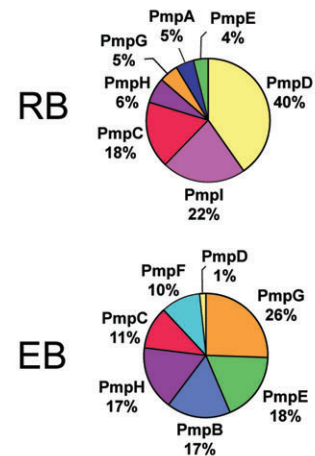
#### The *C. trachomatis* cell envelope

Proteins in the *C. trachomatis* envelope are attractive targets for the development of neutralizing vaccines (Zhang *et al.*, 1987; Peterson *et al.*, 1991; Koehler *et al.*, 1992; Howie *et al.*, 2011). Polymorphic membrane pro-

**Table 1.** Quantitative distribution of functional groups in EB and RB proteomes.

Functional groups	EB – fmol $\mu\text{g}^{-1}$ (rank)	RB – fmol $\mu\text{g}^{-1}$ (rank)
Translation	4661 $\pm$ 45 (1)	6440 $\pm$ 462 (1)
Virulence & T3S-Related	2903 $\pm$ 37 (2)	1310 $\pm$ 115 (6)
Cell Envelope	2463 $\pm$ 31 (3)	3063 $\pm$ 225 (3)
Protein Folding, Assembly & Modification	2362 $\pm$ 72 (4)	3513 $\pm$ 85 (2)
Energy Metabolism	2300 $\pm$ 21 (5)	777 $\pm$ 42 (9)
<i>Chlamydia</i> -Specific Hypothetical Proteins	1503 $\pm$ 28 (6)	1425 $\pm$ 115 (5)
Miscellaneous Enzymes & Conserved Proteins	1449 $\pm$ 37 (7)	1042 $\pm$ 58 (7)
Transcription	1256 $\pm$ 12 (8)	929 $\pm$ 65 (8)
Base & Nucleotide Metabolism	530 $\pm$ 10 (9)	208 $\pm$ 42 (12)
Transport	516 $\pm$ 11 (10)	1494 $\pm$ 70 (4)
DNA Replication, Modification, Repair & Recombination	478 $\pm$ 27 (11)	436 $\pm$ 28 (10)
Central Intermediary Metabolism	182 $\pm$ 7 (12)	58 $\pm$ 2 (15)
Standard Protein Secretion	181 $\pm$ 10 (13)	428 $\pm$ 83 (11)
Amino Acid Biosynthesis	152 $\pm$ 7 (14)	120 $\pm$ 16 (13)
Signal Transduction	112 $\pm$ 5 (15)	32 $\pm$ 6 (16)
Biosynthesis of Cofactors	83 $\pm$ 4 (16)	118 $\pm$ 9 (14)
Cell Division	54 $\pm$ 4 (17)	18 $\pm$ 3 (17)

All *C. trachomatis* L2 proteins quantified were classified into functional categories as described in *Experimental procedures*. The total mass for each category in EB and RB forms was calculated (fmol  $\mu\text{g}^{-1}$ ) and expressed as the mean  $\pm$  standard deviation resulting from four determinations (two biological replicates processed in duplicate). Functional groups were then ranked based on abundance. Protein groups ranked within the top six, representing 76.4% and 80.5% of the total mass in EB and RB, respectively, are highlighted in bold.

**A****B**

**Fig. 4.** Semitryptic peptide analysis indicates that *C. trachomatis* polymorphic membrane proteins (PMPs) are extensively processed. **A.** Semitryptic peptides corresponding to PMPs were analysed and mapped to the corresponding protein sequence. Potential cleavage sites identified are shown (red arrows). Cleavage motif, amino acid position, domains and signal peptides are shown. Signal peptides are indicated based on SignalP 3.0 prediction (<http://www.cbs.dtu.dk/services/SignalP/>) trained for Gram-negative bacterial species. **B.** Pie chart representing the relative abundance of different PMPs in the EB and RB forms, expressed as percentage of total mass corresponding to PMPs.

teins (Pmps) are a diverse group of cell envelope proteins that are postulated to play a role in virulence, immunity and are leading candidates as targets for vaccine development (Longbottom *et al.*, 1998; Grimwood *et al.*, 2001; Crane *et al.*, 2006; Gomes *et al.*, 2006; Tan *et al.*, 2010). All nine Pmps (PmpA to Pmpl) encoded in the *C. trachomatis* genome (Stephens *et al.*, 1998) were identified in our study with their relative abundance varying between developmental forms (Table S1 and Fig. 4B), in agreement with previous studies (Skipp *et al.*, 2005). PmpA and Pmpl were only detected in the RB form whereas PmpF was only detected in the EB form; PmpB, E and G were more abundant in EBs as opposed to PmpC and D, which were more abundant in the RB form, and PmpH was expressed at similar levels in both developmental forms (Table S1). Pmps are classified as autotransporters with an N-terminal passenger domain and a C-terminal  $\beta$ -barrel autotransporter domain that allows translocation of proteins across the bacterial outer membrane (Henderson *et al.*, 2004). The passenger

domain can remain tethered to the outer membrane or be cleaved from the autotransporter domain and secreted (Henderson *et al.*, 2004). We looked for evidence of Pmp processing by searching for semitryptic peptides (peptides not predicted to be generated by trypsin cleavage alone) in our MS/MS analysis, an approach that has been used to delineate proteolytically processed proteins (Thomas *et al.*, 2010). We detected semitryptic peptides that mapped to all Pmps analysed except for PmpA and PmpC. Several of these semitryptic peptides mapped to the predicted signal peptidase cleavage sites – to remove leader sequences of secreted proteins – and to sites adjacent to the autotransporter domain, especially for PmpD–G (Fig. 4A and Table S2). In agreement with these findings, other investigators already suggested that post-translational processing is an important feature of some Pmps. For instance, PmpB and D have been previously shown to be cleaved in *C. trachomatis* (Shaw *et al.*, 2002; Kiselev *et al.*, 2007; 2009) and evidence of Pmps processing has also been found in *C. pneumoniae* (Grim-

wood *et al.*, 2001; Vandahl *et al.*, 2002b). For PmpC we found no semitryptic peptides even though multiple peptides matching this protein were detected (16 in EB and 23 in RB, Table S1). Overall, these findings indicate that all Pmps are expressed, are targets of Sec-dependent transport, and undergo extensive proteolytic processing consistent with their function as autotransporters (Tan *et al.*, 2010). Pmps are major components of the chlamydial outer membrane complex (COMC) and a recent proteomic study has focused on the COMC proteome to reveal new antigens for vaccination (Liu *et al.*, 2010). We found that all proteins classified as being part of the COMC (Liu *et al.*, 2010) were highly expressed in EBs, with MOMP, OmcB, CT623 and PmpG being the most abundant ones (Table S3). This is in agreement with previous reports documenting that these proteins are very abundant in the EB (Caldwell *et al.*, 1981; Hatch *et al.*, 1984; Tanzer and Hatch, 2001; Birkelund *et al.*, 2009; Liu *et al.*, 2010).

#### *Proteins required for mRNA translation, protein transport and protein folding are abundant in the RB form*

Factors required for mRNA translation constituted ~22% of the mass of all proteins quantified in the EB and ~31% in the RB form (Fig. 5A), with the bulk of proteins corresponding to ribosomal proteins (Fig. S2A). Out of 54 ribosomal proteins encoded in the *C. trachomatis* L2 434/Bu genome, 50 were detected in this study (Table S1), with the majority of them being expressed at higher levels in the RB form (Fig. S2B), indicating that the RB devotes a significant proportion of its proteome to actively synthesizing proteins. Factors required for protein folding, assembly and post-translational modifications (chaperones, proteases, peptidases and isomerases – Table S1) were also prominent in the RB form, contributing to ~17% of the proteome, compared with ~11% in the EB (Fig. 5A and Table 1).

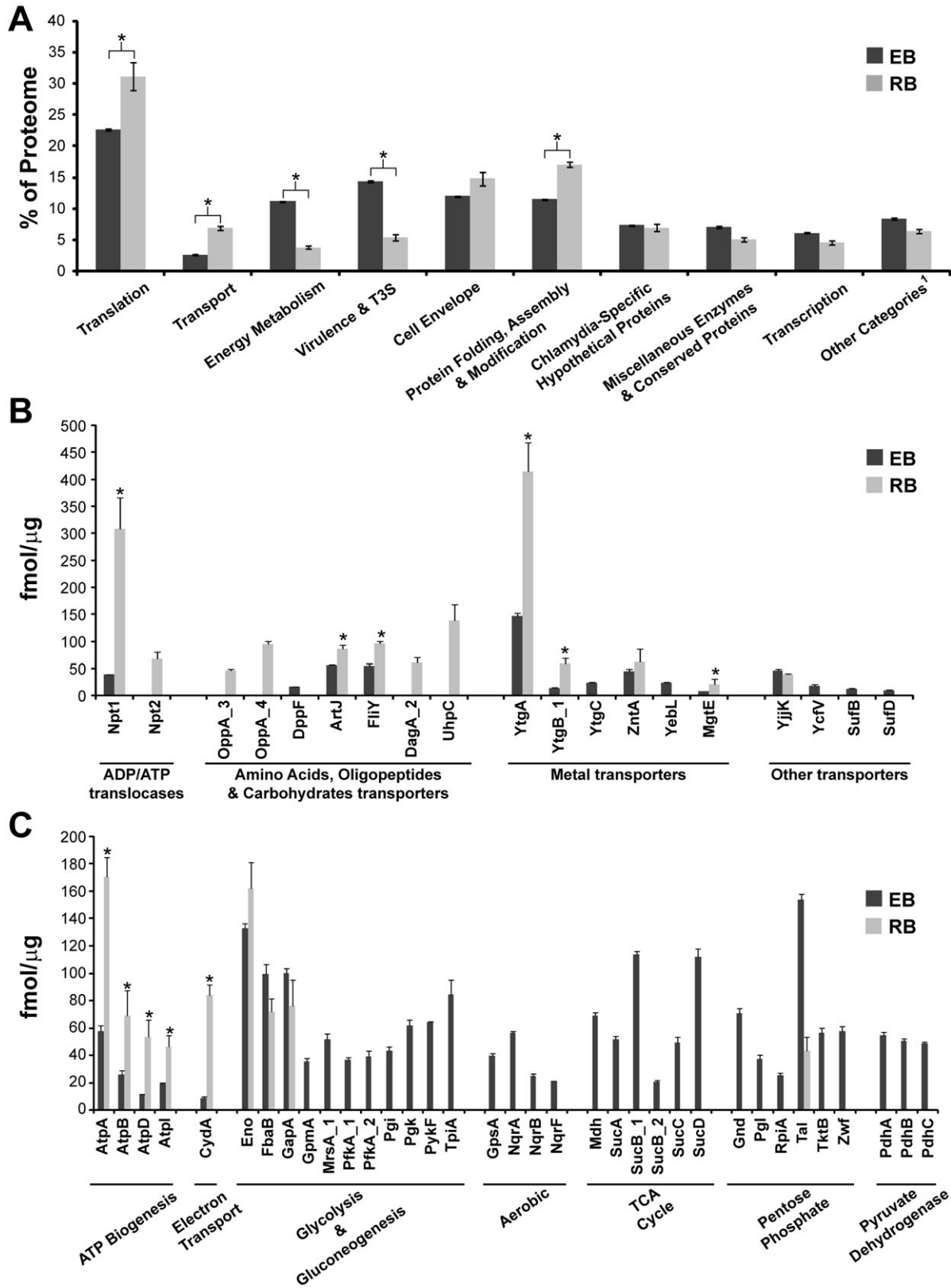
Transporters, permeases and translocators grouped in the 'Transport' category accounted for ~7% of the total mass in the RB form, as compared with ~2.5% in the EB (Fig. 5A). Prominent among this category were nutrient transporters. *C. trachomatis* encodes two integral membrane proteins with ATP/ADP antiporter activity, Npt1 and Npt2 (Stephens *et al.*, 1998; Tjaden *et al.*, 1999). Npt1 mediates the import of host cell ATP coupled with chlamydial ADP export whereas Npt2 has a broader nucleotide transport capacity as it can transport ATP, CTP, GTP and UTP in a proton-dependent manner (Tjaden *et al.*, 1999). Npt1 was approximately eight times more abundant in the RB than in the EB form, and Npt2, while abundant in the RB, was below the detection levels in EBs (Fig. 5B and Table S1).

Amino acid, oligopeptide and sugar transporters were also preferentially found in the RB form. For instance,

OppA\_3 and OppA\_4, OppB\_2 and OppC\_2, components of ABC-type oligopeptides transport systems and YccA (a predicted transporter of unknown substrate), were only detected in RBs (Table S1 and Fig. 5B). A previous proteomics study comparing EB and RB, also detected OppA\_4 only in the RB form (Skipp *et al.*, 2005). Likewise, the Na<sup>+</sup>-linked D-alanine glycine permease DagA\_2 and the hexose phosphate transport protein UhpC, were enriched in the RB form (Fig. 5B). UhpC was also predicted to be enriched in the RB form in a previous transcriptome analysis of *C. trachomatis* (Albrecht *et al.*, 2010). A number of metals transporters including YtgA, a strongly immunogenic periplasmic chlamydial protein (Raulston *et al.*, 2007) possibly involved in iron transport (Miller *et al.*, 2009), were also detected. YtgA and other components of the *ytgAC* operon were considerably more abundant in the RB than in the EB form (Fig. 5B). The overrepresentation of proteins required for ATP, amino acids, oligopeptides, carbohydrate and metal transport is consistent with a high demand for nutrients and cofactors by actively replicating RBs. Overall, the prevalence of ribosomal proteins, nutrient transporters and post-translational processing factors in the RB at 18 hpi is consistent with high metabolic activity in bacteria that are undergoing robust protein synthesis.

#### *The RB accumulates proteins involved in ATP generation*

*Chlamydia trachomatis* encodes a nearly complete tricarboxylic acid (TCA), glycolysis and pentose phosphate pathways for glucose catabolism (Stephens *et al.*, 1998), and possesses the ability to synthesize ATP and generate an ion gradient across the cytoplasmic membrane (Stephens *et al.*, 1998). Several proteins in these pathways, grouped in the 'Energy metabolism' category, were present in EB and RB forms (Table S1). Paradoxically, this cluster of proteins accounted for 3.8% of all proteins in the metabolically active RB as compared with 11.0% in the metabolically 'inert' EB (Fig. 5A), primarily due to higher amounts of proteins required for glucose catabolism in the EB form (Fig. 5C). This ability to use glucose as fuel suggests that the EB is equipped to cope with a high demand for energy at the very early stages post invasion, which has been suggested before by other investigators (Vandahl *et al.*, 2001; Skipp *et al.*, 2005; Sixt *et al.*, 2011). At the RB stage, *C. trachomatis* switches to ATP synthesis by generating an ion gradient. This is likely achieved by using a eukaryotic-like vacuolar (V)-type ATPase, as opposed to the flagellar (F)-type ATPases found in most eubacteria, mitochondria and chloroplasts (Stephens *et al.*, 1998; Dean, 2006). V-type ATPases couple the transfer of protons or sodium ions across cytoplasmic membranes with ATP hydrolysis or synthesis (Forgac,





**Fig. 5.** Quantitative comparison of the EB and RB proteomes.

A. Proteins were grouped into functional categories (as detailed in Table S1) and the total mass for each category was calculated. Values represent the mean contribution of each category expressed as percentage of the total proteome, resulting from four independent MS-based determinations. Error bars represent the standard deviation. Asterisks indicate statistically significant differences ( $P < 0.01$ , Alternate Welch *T*-test not assuming equal standard deviation). All protein categories that individually represented less than 3% of all quantified proteins in both EB and RB were grouped together as 'Other'; these are 'Base & Nucleotide Metabolism', 'DNA Replication, Modification, Repair & Recombination', 'Central Intermediary Metabolism', 'Standard Protein Secretion', 'Amino Acid Biosynthesis', 'Signal Transduction', 'Biosynthesis of Cofactors' and 'Cell Division'.

B and C. Expression levels for individual proteins for which quantitative values could be calculated within the category 'Transport' (B) and 'Energy Metabolism' (C) are represented and expressed as the mean ( $\text{fmol } \mu\text{g}^{-1}$ ) resulting from four independent mass spectrometry-based determinations. Subcategories are indicated. Error bars indicate the standard deviation. Asterisks indicate statistically significant differences ( $P < 0.05$ , Alternate Welch *T*-test not assuming equal standard deviation).

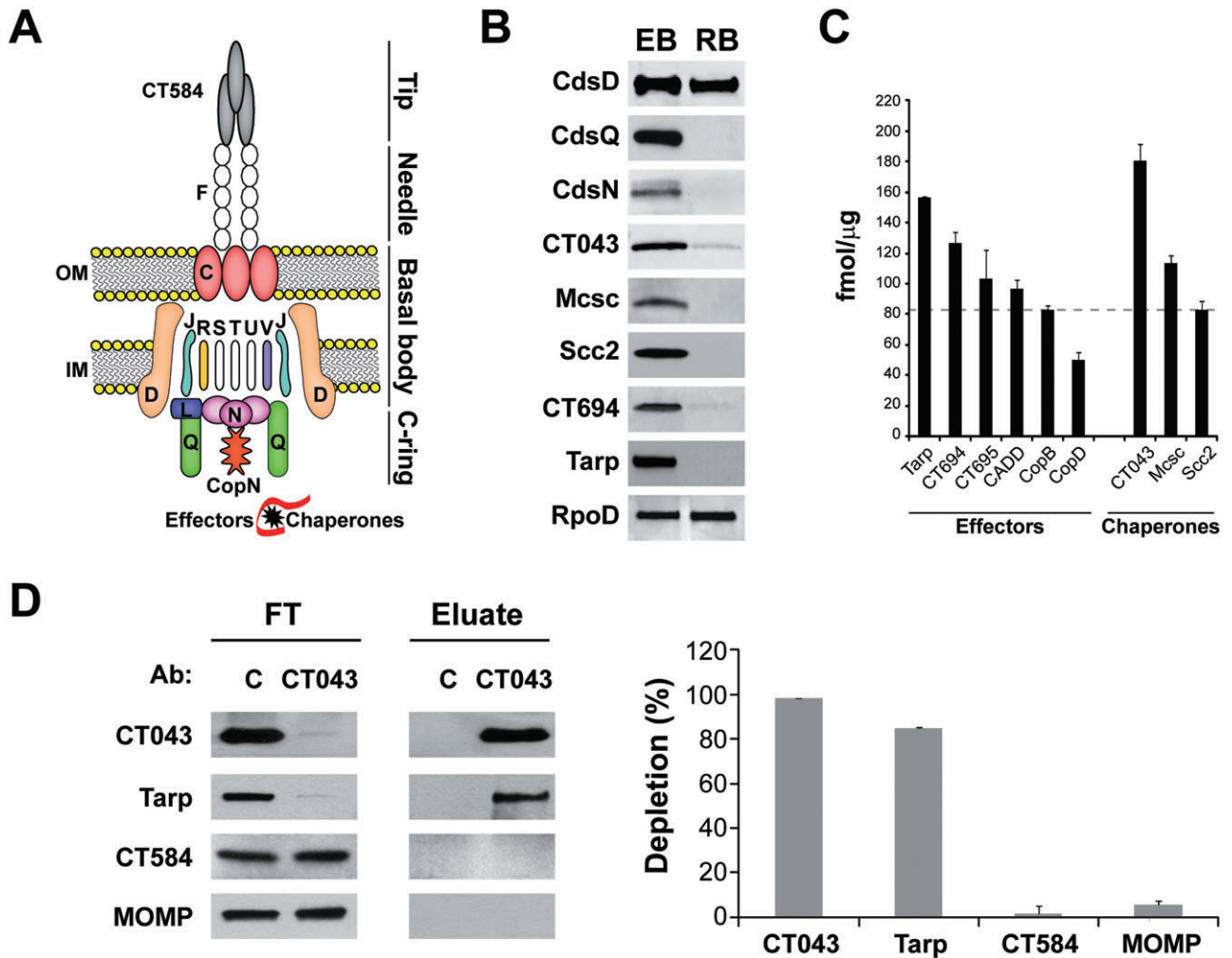
2007). Whereas in eukaryotic cells these enzymes are primarily involved in generating proton gradients across membranes, prokaryotic V-type ATPases are responsible for ATP synthesis (McClarty, 1999; Numoto *et al.*, 2009). All six predicted V-type ATPase subunits (AtpA, AtpB, AtpD, AtpE, AtpI and AtpK) were expressed in both the EB and RB forms (Table S1) but at higher levels in latter (Fig. 5C). Consistent with this, components of the cytochrome *bd* respiratory oxidase (e.g. CydA) (McClarty, 1999), which presumably helps transfer protons to reduce oxygen, were more abundant in the RB (Fig. 5C). Overall, these findings indicate that replicating RBs generate ample pools of ATP both through transport from the host and through synthesis. This excess of ATP may fuel the replication of bacteria but also may account for the observation that EBs possess a large depot of stored ATP (Tipples and McClarty, 1993). Presumably ATP synthesis ramps up as the RB begins its transition to the EB form, and provides the invasive form of the bacterium with the fuel required to drive protein secretion during invasion, nascent inclusion biogenesis and to prime the developmental transition to the RB form.

#### *The EB is pre-loaded with an abundant arsenal of type III secretion effectors and chaperones*

We observed significant differences in 'Virulence & T3S' proteins between EB and RB forms. This protein group represented ~14% of the EB proteome as opposed to ~5% in the RB (Fig. 5A). Most proteins within this group were related to type III secretion (T3S) system in both EB and RB (Table S1). The T3S apparatus is a conserved syringe-like multi-protein structure used by Gram-negative bacteria to inject protein effectors into eukaryotic host cells and as such, a functional T3S system is essential for virulence (Galan and Wolf-Watz, 2006; Beeckman and Vanrompay, 2010). The *Chlamydiaceae* encode a complete set of T3S genes (Hefty and Stephens, 2007; Peters *et al.*, 2007), and assemble a T3S apparatus with a proposed architecture similar to that of other bacterial pathogens (Beeckman and Vanrompay, 2010; Betts-Hampikian and Fields, 2010). We identified most structural T3S components (Fig. 6A), 25 predicted T3S

effectors and 7 T3S chaperones (Table S1). As shown in Fig. 6B, we verified our proteomics results by immunoblot analysis of a subset of T3S effectors (Tarp, CT694), T3S components (basal body component CdsD and cytoplasmic accessory factors CdsQ and CdsN) and chaperones (Mscs, CT043, Scc2). T3S chaperones and empirically verified T3S effectors in EBs were among the top 25% most abundantly expressed proteins (Fig. 6C). T3S chaperones stabilize secreted effectors, provide signals for efficient secretion and partially unfold effectors for translocation through the T3S needle (Yip *et al.*, 2005). High expression of T3S chaperones is consistent with proposed models where EBs are preloaded with abundant T3S effectors (Peters *et al.*, 2007). We determined that Tarp, an effector essential for invasion (Jewett *et al.*, 2010), was the most abundant T3S effector and CT043 (Spaeth *et al.*, 2009) was the most abundant putative T3S chaperone (Fig. 6C) in EBs. We tested the hypothesis that the most abundant T3S chaperone would bind to the most abundant effector by immunoprecipitating CT043 from EB total lysates and assessing the degree of Tarp co-immunoprecipitation. Anti-CT043 antisera depleted both CT043 and Tarp from EB lysates, but not CT584, an abundant predicted T3S needle-tip protein (Markham *et al.*, 2009), or the major outer membrane protein MOMP (Fig. 6D), underscoring that most Tarp in the EB is in complex with CT043. Similar results have been obtained for other abundant T3S effectors (Y. Chen and R.H. Valdivia, unpublished).

Interestingly, when we analysed the expression levels of T3S components, we found that whereas CdsD, a component of the basal body (Johnson *et al.*, 2008), was equally abundant in the RB and EB forms, two components that are peripherally associated with the T3S basal apparatus, the C-ring component CdsQ (Johnson *et al.*, 2008) and the ATPase CdsN (Stone *et al.*, 2008), were largely absent in the RB (Table S1 and Fig. 6B). In *Shigella* the C-ring component Spa33/SpaO and the ATPase Spa47 are required for the assembling of the needle and for the export of T3S effectors (Jouihri *et al.*, 2003; Morita-Ishihara *et al.*, 2006). Both the C-ring component and the ATPase have been proposed to act as recognition platforms for T3S substrates (Beeckman and Vanrompay,



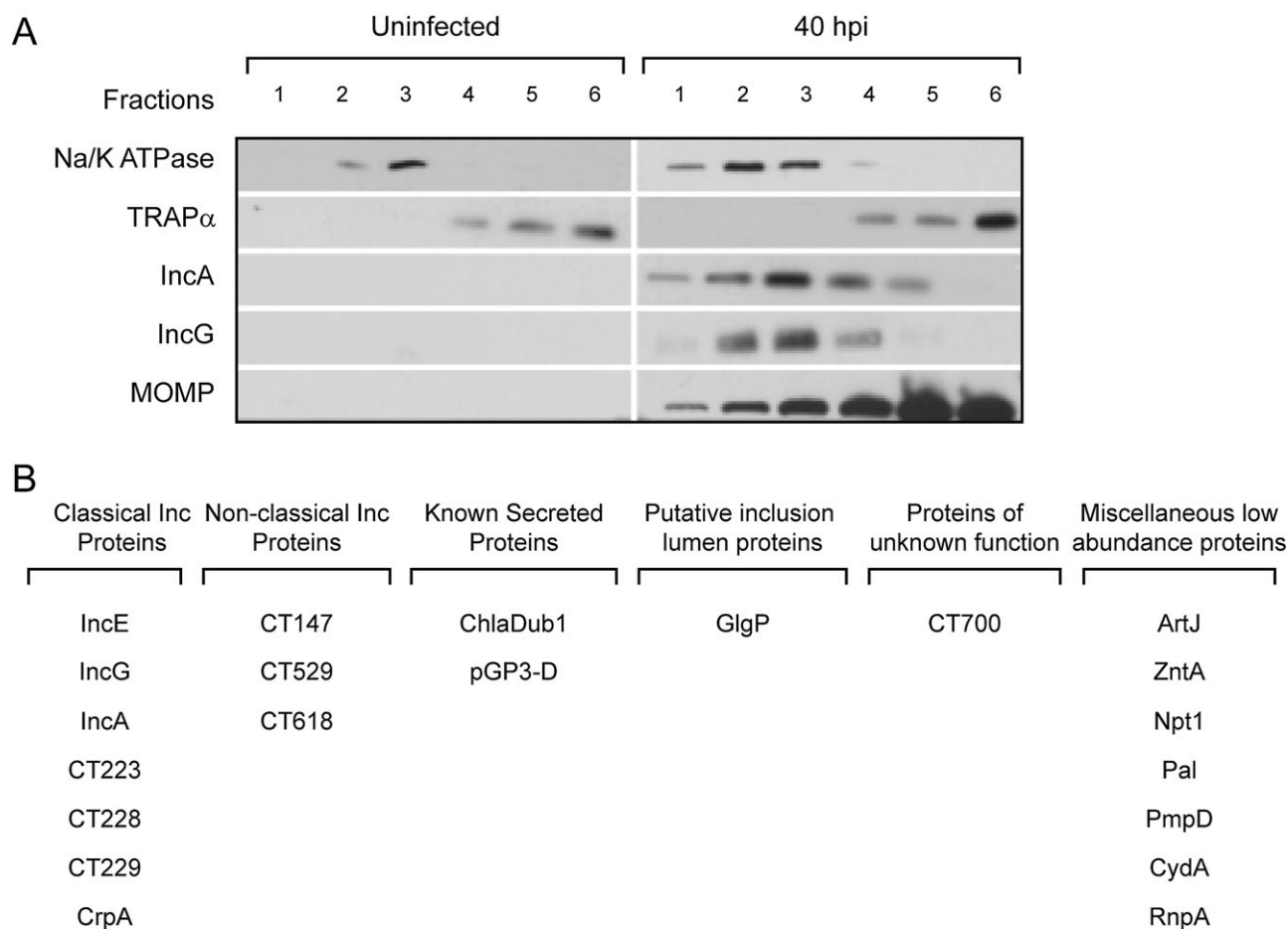
**Fig. 6.** T3S chaperones, cytoplasmic accessory factors and effectors are abundant in the EB form.

A. Cartoon displays a schematic representation of the chlamydial T3S system (Betts-Hampikian and Fields, 2010). Cds proteins are shown with letter designation only. Proteins for which expression was detected are shown in colour. OM: outer membrane. IM: inner membrane. B. Comparison of expression levels for selected T3S components (basal body component CdsD and cytoplasmic accessory factors CdsQ and CdsN), chaperones (Mcsc, CT043, Scc2) and effectors (Tarp, CT694) between EB and RB forms, as determined by immunoblots. C. Expression levels for recognized T3S effectors and chaperones in EBs are represented as the mean ( $\text{fmol } \mu\text{g}^{-1}$ ) resulting from four independent mass spectrometry-based determinations. Dotted line indicates the 75th percentile for the EB proteome ( $82.5 \text{ fmol } \mu\text{g}^{-1}$ ), highlighting that the shown effectors and chaperones rank in the top 25% of proteins by abundance. Error bars indicate the standard deviation.

D. The most abundant chaperone, CT043, is associated with the most abundant T3S effector, Tarp. Immunoblots correspond to immunoprecipitation experiments using rabbit-raised anti-CT043 antibody. The flow-through (FT) and the bound material (Eluate) obtained after incubating EB lysates with beads cross-linked with either pre-immune serum (used as a control, C) or anti-CT043 sera, were blotted for CT043, Tarp, CT584 and MOMP (left panel). Quantitative immunoblots show the % depletion of Tarp, CT043, CT584 and MOMP compared with controls, after incubation with anti-CT043 cross-linked beads (right panel). Note co-depletion of Tarp by anti-CT043 antibodies. Result is representative of at least three independent experiments.

2010). Similarly, in the flagellar T3S system, the C-ring is required for proper assembly of the flagellum (Gonzalez-Pedrajo *et al.*, 2006) and both the ATPase and the C-ring have been proposed to increase the efficiency of secretion of flagellar substrates (Konishi *et al.*, 2009; Erhardt and Hughes, 2010). The relative absence of the cytoplasmic accessory factors CdsQ and CdsN in the RB forms suggest that additional factors may substitute for these components, as has been suggested for flagellar T3S

system (Konishi *et al.*, 2009; Erhardt and Hughes, 2010). The CdsN homologue CT717 could potentially substitute for CdsN at this stage. However, we were unable to detect CT717 by MS in either developmental form. Given that T3S chaperones are also markedly absent in RBs, an alternative interpretation for the absence of CdsQ and CdsN is that the RB stage has a reduced T3S capacity or that the number of active T3S apparatus is limited. Yet, we should highlight that this is unlikely to have an impact on



**Fig. 7.** Identification of *C. trachomatis* proteins associated with inclusion membranes.

A. Immunoblots showing fractionation of total membranes extracted from uninfected cells and from cells infected with *C. trachomatis* L2 (40 h post infection). Na/K ATPase and TRAP $\alpha$  were used as markers for plasma and endoplasmic reticulum membranes respectively. IncA and IncG were used as markers for inclusion membranes and MOMP indicates the fractions enriched in intact bacteria. Proteins from fractions 2 and 3, which were enriched for IncA and IncG, were extracted and analysed by LC-MS/MS.

B. Compendium of *C. trachomatis* L2 proteins associated with inclusion membranes. We highlight previously identified inclusion membrane proteins (Li *et al.*, 2008a) and proteins not abundant in EBs.

secretion of non-T3S factors by RBs. Our results suggest that the RB can devote more resources to increase bacterial numbers and cellular mass by sharing the task of synthesizing and secreting virulence factors. As each RB begins its transition to the IB (~20 hpi for *C. trachomatis* L2), we postulate that the synthesis of CdsQ, CdsN, T3S chaperones and EB-specific effectors ramps up to pre-pack the future EBs with these secretion enhancers.

#### Inclusion membrane proteomics

In addition to the EB and RB forms, the inclusion membrane itself is heavily modified by *Chlamydia*-derived proteins (Moorhead *et al.*, 2010), representing a poorly explored subset of the chlamydial proteome in infected cells. Prominent among these are Inc proteins, putative T3S substrates that share a common bi-lobed hydropho-

bic motif predicted to direct their insertion into the inclusion membrane (Bannantine *et al.*, 2000). To identify chlamydial proteins at the inclusion membrane, we fractionated membranes from infected cells on isopycnic density gradients and monitored fractions enriched for the well-characterized inclusion membrane proteins IncA and IncG (Li *et al.*, 2008a) (Fig. 7A). Total proteins were extracted from these fractions and subjected to LC-MS/MS analysis. Although the bulk of proteins (> 99%) were of human origin, we were able to identify a number of chlamydial proteins which likely represent the top abundant proteins associated with the inclusion membrane. Within the chlamydial proteins identified, a small group of proteins expressed at very high levels in the EB form (mainly the components of the chlamydial outer membrane complex MOMP, PmpG and CT623, the T3S component CdsD, the hypothetical protein CT875, the ABC

transporter *ytgA*/CT067, few translation and initiation factors and one ribosomal protein – data not shown) were considered likely contaminants and removed from the analysis. This led to a final list of 21 chlamydial proteins over-represented in IncA/IncG enriched membrane fractions (Fig. 7B). As expected, most proteins in this group consisted of predicted inclusion membrane proteins. In addition, we detected known secreted proteins like the virulence plasmid protein pGP3-D (Li *et al.*, 2008b) and the predicted T3S effector ChlaDub1/CT868 (Jehl *et al.*, 2011), along with GlgP/CT248 involved in glycogen metabolism. Also, a number of miscellaneous proteins of low abundance in the EB but enriched in inclusion membrane fractions were detected, as detailed in Fig. 7B. These included PmpD, which was not identified as being enriched in the *Chlamydia* outer membrane complex in a recent publication (Liu *et al.*, 2010), thus unlikely a contaminant in our inclusion membrane preparations. A surprising finding from this analysis is the presence of periplasmic and cytosolic membrane proteins in association with inclusion membrane fractions. These include an arginine transporter (ArtJ/CT381), a metal transporter (*zntA*/CT727), the ATP/ADP translocase (Npt1/CT065) and the cytochrome oxidase subunit I (CydA/CT013). Whether the enrichment of these proteins in the inclusion membrane fraction is non-specific or they perform scavenging functions in the inclusion lumen or in association with inclusion membranes, remains to be determined.

### Conclusions

*Chlamydia trachomatis*, a pathogen with high impact on human health, has been experimentally difficult to study as traditional genetic and physiological approaches have been of limited use. With a quantitative proteomic approach, we provided molecular evidence of the different metabolic and virulence properties of the two developmental stages of *C. trachomatis*. We developed an approach to overcome the quantitative biases that arise from different levels of contamination of EB and RB extracts with host cell proteins. This approach can be applied to other studies where quantitative proteomics is carried out in the context of 'mixed-proteomes', such as host–pathogen and host–symbiont interactions.

It is important to note that for our proteomic study, the RB form was purified at 18 hpi, a stage at which RB replication is logarithmic and contamination with EB form (due to the asynchronous nature of EB to RB transition and eventually to a low number of dead EBs) is minimal (Nicholson *et al.*, 2003). Our findings on RBs at this stage may not apply to RB forms at other stages of infection. The isolation and characterization of RB forms at different stages of infection for longitudinal studies is limited by the ability to isolate a pure popula-

tion of these fragile *Chlamydia* forms and by the detection limits of current mass spectrometers. However, at the current rate of advances in MS-based detection and quantification methods such analysis may soon be possible.

Our quantitative proteomics study provided experimental confirmation for what had been suggested in transcriptional studies (Nicholson *et al.*, 2003). The RB form at 18 hpi was found to be primarily primed for robust protein synthesis, nutrient transport and the accumulation of ATP. Thus, the proteome of the RB at this stage is specialized for efficient replication and for the imminent transition to the EB form. In contrast, the EB is primed for high T3S capacity and for generating a burst of energy via glucose catabolism to fuel the EB to RB developmental transition. A novel observation from these studies is the relative lack in the RB form of T3S chaperones and cytoplasmic accessory factors required for efficient recognition of T3S substrates (Jouihri *et al.*, 2003; Morita-Ishihara *et al.*, 2006; Beeckman and Vanrompay, 2010). One possible interpretation of our findings is that as the EB transitions to the RB form there is a progressive reduced capacity in chaperone-assisted T3S by each individual RB. As infection progresses the need for T3S effector translocation could be incrementally compensated by the growing numbers of RBs within one inclusion. This would allow individual RBs to save resources for replication and EB generation and prevent a potential excess of T3S effectors from being secreted by exponentially increasing numbers of RBs. Such excess of effectors could harm the host cell, disrupt the development of the inclusion or provide substrates for antigen presentation by the infected cell.

### Experimental procedures

#### *Culture conditions and purification of C. trachomatis EB and RB forms*

*Chlamydia trachomatis* biovar LGV, serotype L2, strain 434/Bu was propagated in HeLa CCL2 monolayers (ATCC, Rockville, Maryland, USA) grown in Dulbecco's minimal essential medium (DMEM high glucose 1×) (Gibco/Invitrogen Life Technologies, Carlsbad, California, USA) supplemented with 10% fetal bovine serum (Mediatech, Manassas, Virginia, USA) at 37°C, 5% CO<sub>2</sub> in a humidified atmosphere. Infections were carried out in T175 flasks (Sarstedt, Nümbrecht, Germany) by adding a suspension of EBs at a multiplicity of infection (moi) of 10. *C. trachomatis* RB and EB forms were collected at 18 and 44 hpi respectively. Purification of *C. trachomatis* EBs and RBs was performed by density gradient centrifugation essentially as previously described (Caldwell *et al.*, 1981) with minor modifications. Briefly, Renografin was replaced by Omnipaque 350 (GE Healthcare, Princeton, New Jersey, USA) supplemented with NaCl 160 mM. The gradients were prepared by diluting Omnipaque

350–160 mM NaCl in SPG buffer (3.8 mM  $\text{KH}_2\text{PO}_4$ , 7.2 mM  $\text{K}_2\text{HPO}_4$ , 4.9 mM L-glutamic acid, 218 mM sucrose, pH = 7.4) such that final concentrations of Omnipaque 350 were 28.5%, 38.0%, 41.8% and 51.3% in successive layers. To assure purity of LGV-L2, the strain was plaque purified twice (O'Connell and Nicks, 2006) before generating EB and RB forms used for proteomic analysis. All strains and cell lines were *Mycoplasma*-free as determined by a previously described PCR method (van Kuppeveld *et al.*, 1992).

#### Preparation of *C. trachomatis* total protein extracts and normalization strategy

To prepare total protein extracts for LC/LC-MS/MS, EBs or RBs were suspended in lysis buffer (20 mM Tris-HCl pH 8.0, 5 mM EDTA, 50 mM NaCl, 15 mM DTT, 0.06 mM 2-Mercaptoethanol, 1 mM  $\text{Na}_3\text{VO}_4$ , 50 mM NaF, 100 mM  $\text{NH}_4\text{HCO}_3$ , 0.5% RapiGest SF Surfactant [Waters Corp., Milford, Maryland, USA] in 100 mM  $\text{NH}_4\text{HCO}_3$ ), briefly sonicated on ice, heated at 65°C for 10 min and then boiled for 5 min in water. Lysates were centrifuged at 25 000 *g* (10 min, 4°C) to remove insoluble debris and supernatants were stored at -80°C. Total protein content in the extracts was estimated by Bradford assay (Bradford, 1976). To visualize the band pattern (Fig. S1D), 20 µg of EB and RB protein extracts were loaded onto SDS-PAGE 4–15% gradient gels (Bio-Rad, Hercules, California, USA) and stained with SYPRO Orange (Invitrogen Life Technologies, Carlsbad, California, USA), scanned in a Typhoon 9410 Variable Image Phosphor Imager and processed with ImageQuant 5.2 (GE Healthcare, Princeton, New Jersey, USA). For two preparations each of EB and RB samples, a total of 53 µg and 16.5 µg of protein respectively was digested with trypsin: briefly, samples concentrations were normalized to approximately 1 µg µl<sup>-1</sup> (using BSA-calibrated Bradford assay) in 50 mM ammonium bicarbonate supplemented with 0.25% v/v RapiGest SF Surfactant (Waters Corp., Milford, Maryland, USA). Protein was reduced with 10 mM dithiothreitol at 80°C for 15 min, alkylated with 20 mM iodoacetamide at room temperature in the dark for 1 h, and digested with trypsin (20 ng µg<sup>-1</sup>, Promega Gold) overnight at 37°C. RapiGest SF Surfactant (Waters Corp., Milford, Maryland, USA) was hydrolysed with the addition of trifluoroacetic acid to 0.5% v/v final and heating at 60°C for 2 h. The samples were then diluted 1:1 with 200 mM ammonium formate (pH 10.0) to raise the pH to 10. Six microlitres of injections (approximately 3 µg of protein) were utilized for LC/LC-MS/MS analysis. We took into account the different proportion of human content in both samples (as detailed in *Protein quantification by mass spectrometry*) and calculated the yield of bacterial proteins in EB and RB extracts. To normalize these samples on a 'per organism' basis, serial dilutions of gradient-purified EBs and RBs were suspended in 1× PBS, stained with Bodipy TR C5 Ceramide (BODIPY TR) following manufacturer's instructions (Invitrogen Life Technologies, Carlsbad, California, USA), and the numbers of bacteria per µl in EB and RB suspensions used to prepare protein lysates were determined by fluorescence microscopy and DIC microscopy and referred to protein concentration obtained in EB and RB extracts. The 'mass per particle' values obtained for EB and RB forms were very similar (34.3 and 37.9 fg per particle respectively), allow-

ing for a direct comparison of protein quantitative values (expressed as fmol µg<sup>-1</sup> of chlamydial protein) between EB and RB samples.

#### Antibodies, Western blot and immunoprecipitations

Anti-CT288, -CT694, -CT584, -CdsQ and -Tarp antibodies were generated in our laboratory by immunization of female White New Zealand rabbits with GST-purified fusions expressed in *E. coli* as previously described (Spaeth *et al.*, 2009). Rabbit polyclonal anti-CT043, -CdsN, -Scc2 and -Msc antibodies were also generated in our laboratory using recombinant His-tagged proteins. Additional antisera include: rabbit polyclonal anti-IncA (Cocchiario *et al.*, 2008), anti-MOMP and anti-CdsD (K. Fields, University of Miami, USA); anti-RpoB and anti-RpoD (M. Tan, UC Irvine, USA); anti-Hc1 and anti-IncG (T. Hackstadt, Rocky Mountains Laboratories, USA); anti-PmpD (fraction 2) (M. Lampe, University of Washington, USA), anti-OmcB (T. Hatch, University of Tennessee Health Science Center, USA), anti-TRAPα (C. Nicchitta, Duke University) and mouse monoclonal anti-Na-K ATPase (hybridoma bank, University of Iowa, USA). For Western blots, protein extracts were loaded onto SDS-PAGE 4–15% gradient gels, transferred to 0.45 µm nitrocellulose membranes using a Trans-Blot SD Semi-Dry Electrophoretic Transfer Cell (Bio-Rad, Hercules, California, USA), blocked in 5% non-fat powder milk in TBST (50 mM Tris-Base, 150 mM NaCl, 0.1% Tween 20 pH 7.4) and incubated with primary antibodies diluted in 5% non-fat powder milk in TBST, followed by incubation with goat anti-rabbit secondary antibodies conjugated to horseradish peroxidase (Sigma-Aldrich, St. Louis, Missouri, USA). A chemoluminescence reaction (Pierce, Rockford, Illinois, USA) and ECL-hyperfilm (GE Healthcare, Princeton, New Jersey, USA) were used to detect immunoreactive material. Immunoprecipitation assays were performed using Pierce Crosslink Immunoprecipitation Kit (Pierce, Rockford, Illinois, USA). IgGs against CT043 or pre-immune sera were cross-linked to protein A/G resins according to manufacturer's instructions. Approximately  $5 \times 10^9$  inclusion forming units of EBs were lysed in Pierce IP lysis buffer (1% Nonidet P40, 5% glycerol in TNE pH 7.4) supplemented with EDTA-free protease inhibitor cocktail (Roche, Basel, Switzerland), 1 mM DTT and 1 mM PMSF. After sonication, lysates were cleared by centrifuging at 25 000 *g* (10 min, 4°C) and the supernatants were then incubated with IgG- resins for 2 h at 4°C. Bound proteins were eluted with Pierce elution buffer (pH 2.8). Lysates after binding were also collected (flow-through, FT). Both samples were subjected to SDS-PAGE electrophoresis and analysed by Western blot. The percentage of depletion in the FT versus control was calculated in quantitative Western blots carried out essentially as described above but using Alexa Fluor 680-labelled goat anti-Rabbit (Invitrogen Life Technologies, Carlsbad, California, USA) as secondary antibody and developing the membranes in a LI-COR Odyssey instrument (Lincoln, New England, USA).

#### Microscopy

Gradient-purified EBs and RBs were fixed onto glass coverslips with 2% formaldehyde–0.025% glutaraldehyde. For indi-

rect immunofluorescence, fixed EBs and RBs were blocked with 5% bovine serum albumin (BSA) in phosphate buffer saline solution (PBS) and incubated with polyclonal anti-MOMP antibody on ice for 1 h. Immunoreactive material was detected with Alexafluor-conjugated secondary antibodies (Invitrogen Life Technologies, Carlsbad, California, USA). Coverslips were mounted in Mowiol mounting medium and images were acquired with a Leica TCS SL confocal microscope and processed with Leica imaging software. Gradient-purified EBs and RBs were also suspended in 1× PBS and stained with Bodipy TR C<sub>5</sub> Ceramide (BODIPY TR) following manufacturer's instructions (Invitrogen Life Technologies, Carlsbad, California, USA). Fluorescent and differential interference contrast microscopy images of BODIPY TR-stained EBs and RBs were acquired with a Zeiss Axioscope epifluorescence microscope equipped with a Hamamatsu CCD camera and processed with Axiovision v3.0 imaging software.

#### LC-MS data collection

Peptide digests from each of the samples (EB and RB) were analysed using a nanoAcquity UPLC system with 2D Technology coupled to a Synapt HDMS mass spectrometer (Waters Corp, Milford, MA), using a method which generated five fractions at pH 10 with approximately equal loading in each fraction, similar to previously described (Gilar *et al.*, 2005a,b; Dowell *et al.*, 2008). Approximately 3 µg of digested EB or RB sample was first trapped at 2 µl min<sup>-1</sup> at 97/3/0.1 v/v/v water/acetonitrile (MeCN)/formic acid on a 5 µm XBridge BEH130 C18 300 µm × 50 mm column. Four-minute steps at 2 µl min<sup>-1</sup> to the following % MeCN were used to generate the five fractions at pH 10, with the composition returning to 97/3/0.1 composition during the analytical second dimension: 10.8%, 14.0%, 16.7%, 20.4% and 65.0%. At each condition, the flow-through from the first dimension was diluted online 10-fold with 99.8/0.1/0.1 v/v/v water/MeCN/formic acid and trapped on a 5 µm Symmetry C18 300 µm × 180 mm trapping column. Separations for each fraction were then performed on a 1.7 µm Acquity BEH130 C18 75 µm × 250 mm column (Waters) using a 90 min gradient of 5–40% MeCN with 0.1% formic acid at a flow rate of 0.3 µl min<sup>-1</sup> and 45°C column temperature. We conducted one five-fraction data-independent analysis (MS<sup>E</sup>) analysis and one five-fraction data-dependent analysis (DDA) of each sample (two EB and two RB), for a total of eight sample injections and forty 90 min LC-MS acquisitions. MS<sup>E</sup> runs of samples obtained from different sections were performed in random order, and used 0.9 s cycle time alternating between low collision energy (6 V) and high collision energy ramp (15–40 V). The DDA mode utilized a 0.9 s MS scan followed by MS/MS acquisition on the top three ions with charge greater than 1. MS/MS scans for each ion used an isolation window of approximately 3 Da, a maximum of 4 s per precursor, and dynamic exclusion for 120 s within 1.2 Da of the selected precursor.

#### LC-MS data processing

For the purposes of label-free peptide quantification, EB and RB samples were processed independently because of the

large difference in sample composition. For robust peak detection and label-free alignment across sample injections (20 for EB and 20 for RB), the commercial package Rosetta Elucidator v3.3 (Rosetta Biosoftware, Seattle, WA) with multidimensional PeakTeller algorithm was utilized, in a similar manner to a number of recent publications (Meng *et al.*, 2007; Paweletz *et al.*, 2010). Alignment between samples across each fraction is accomplished first, followed by summation of the five fractions to obtain aggregate data for each sample. Feature intensities for each injection were subjected to robust median scaling (top and bottom 10% excluded) to generate a single intensity measurement for each feature (accurate mass and retention time pair) in each sample. As previously reported (Dowell *et al.*, 2008), the High/Low pH RPLC configuration generated highly unique fractions, with 89% and 87% of peptides eluting in only a single fraction for EB and RB samples respectively.

We utilized both DDA and MS<sup>E</sup> to generate peptide identifications. For DDA acquisition files.mgf searchable files were produced in Rosetta Elucidator and searches were then submitted to and retrieved from the Mascot v2.2 (Matrix Sciences) search engine in an automated fashion. For MS<sup>E</sup> data, ProteinLynx Global Server 2.4 (Waters Corporation) was used to generate searchable files which were then submitted to the IdentityE search engine (Waters Corporation, Milford, MA) (Geromanos *et al.*, 2009; Li *et al.*, 2009). Results files were then imported back into Elucidator. A total of 96 306 and 73 222 rank 1 search results were obtained for the EB and RB samples respectively. To enable global spectra scoring across results from both search engines, all search results were concurrently validated using the PeptideProphet and ProteinProphet algorithms in Elucidator using independent reverse decoy database validation (Keller *et al.*, 2002; Nesvizhskii *et al.*, 2003). The PeptideProphet score was set such that the aggregate data set has a 1% peptide FDR, which corresponded to a score of 0.77 and 0.82 for EB and RB data sets respectively. Each peptide identified was allowed to be assigned to a single protein entry, and these assignments were made by ProteinProphet according to the rules of parsimony. For the EB samples there were 754 human peptides and 3916 chlamydial peptides identified, and 14 peptides identified which were in both human and chlamydia databases. For the RB samples there were 4025 human peptides and 1274 chlamydial peptides identified, and eight peptides shared between human and chlamydia databases.

Both DDA and MS<sup>E</sup> data were searched against an aggregate database of Swissprot *human* (<http://www.uniprot.org>, 20328 unique entries) and NCBI *Chlamydia* (<http://www.ncbi.nlm.nih.gov/pubmed/>, 5063 unique entries), both downloaded on 24 September 2009. Full *Chlamydia* database was utilized as opposed to only *C. trachomatis* L2 434/Bu to enable the possibility of detecting proteins not yet placed in the L2 434/Bu-specific database, or detecting additional amino acid substitutions not yet sequenced in the strain. The database was appended with full 1× reverse database for peptide false discovery rate determination, and duplicates were removed using Protein Digest Simulator Basic (<http://omics.pnl.gov/software>). Precursor ion mass tolerance was 20 ppm for both PLGS and Mascot searches, and product ion tolerance was 0.04 Da for Mascot and 40 ppm for PLGS. Enzyme specificity was set to tryptic for Mascot and PLGS

2.4 searches, with the exception of the specific semitryptic data analysis, which utilized only the DDA data files for Mascot semitryptic enzyme searches. A maximum of two missed cleavages were allowed. Carbamidomethyl cysteine was included as a fixed modification, and variable modifications included oxidized methionine and deamidated asparagine and glutamine.

#### LC-MS data quality control

Data quality control for the 20 analyses of each sample type was performed within the Rossetta Elucidator software package using principal components analysis (PCA). Three-dimensional PCA indicated excellent reproducibility and tight grouping of technical replicates both for EB and RB samples (Fig. S3).

#### Protein quantification by mass spectrometry

We employed a novel adaptation of the previously described 'absolute quantification' approach (Delahunty and Yates, 2005; Silva *et al.*, 2006b), with several modifications to address mixed-species proteomic samples. First, peptides identified that are homologous between *Chlamydia* and human are removed, as the species origin of these peptides cannot be defined ( $n = 14$  peptides in EBs,  $n = 8$  peptides in RBs). Next, the peptides were ranked according to their average intensity across the study and the average intensity of the top three peptides for each protein was calculated as a measurement of each protein's relative abundance in the sample, as previously described (Silva *et al.*, 2006b). We also calculate this average for proteins with two peptides to match, which also gives a reasonable estimation of protein abundance (Reidel *et al.*, 2011), and is necessary because of the low molecular weight of many *Chlamydia* proteins. Proteins with only one peptide to match were eliminated from the quantitative analysis. Next, based on the historic response factor of the instrument utilized ( $2050 \pm 400$  counts  $\text{fmol}^{-1}$ ,  $n = 117$ ) we calculated the fmol of each protein in the sample. Using each protein's molecular weight from the database, this fmol quantity was converted to nanograms, and by summing these values for each analysis we calculate the total ng in each sample. The total protein loading calculated in this manner is highly comparable to the  $3 \mu\text{g}$  measured by BSA-calibrated Bradford assay for each sample; the EB value was  $2760 \pm 160$  ng for four analyses and RB value was  $2570 \pm 170$  ng for four analyses. The average *Chlamydia* protein content in EB was  $2450 \pm 290$  ng (89%) and in RB was  $578 \pm 94$  ng (22%). Finally, to calculate the species-specific protein expression for each sample, the fmol value for each protein was divided by the ng sum for only the species of interest, and scaled by 1000 to yield  $\text{fmol } \mu\text{g}^{-1}$ . The  $\text{fmol } \mu\text{g}^{-1}$  and standard deviation across four measurements for all proteins in EB and RB are reported in Table S1. This quantitative procedure was vetted prior to deployment on EB/RB samples using a model system where an *E. coli* lysate (Waters MassPrep) was differentially spiked with exogenous proteins (MassPrep Standard yeast enolase, bovine albumin, yeast alcohol dehydrogenase and rabbit glycogen phosphorylase) in predefined ratios (Fig. 2). One of the samples was

then mixed 50/50 with mouse brain lysate digest, and  $1 \mu\text{g}$  total of each sample was analysed in triplicate by single dimension LC-MS/MS. Instrumentation and quantitative methodology was identical to described above, except only a single dimension of separation was used. Figure 2 shows that without species-specific correction (i.e. using sum of all protein ng as denominator to express  $\text{fmol } \mu\text{g}^{-1}$  quantity), there is a systematic bias against the *E. coli* and spiked-in proteins. Nevertheless, this bias was efficiently removed when the 'species-specific' correction was applied.

#### Purification and proteomics analysis of inclusion membrane proteins

HeLa cells were infected with L2 434/Bu EBs (moi  $\sim 10$ ) for 40 h and harvested in Hanks balanced salt solution (HBSS) containing complete EDTA-free protease inhibitor cocktail (Roche, Basel, Switzerland) and 2 mM PMSF. The cell suspension was sonicated at 50 watts (three times, 30 s) and the cell lysate centrifuged at  $500 g$  for 10 min at  $4^\circ\text{C}$ . The post nuclear supernatant was then transferred to ultra-clear ultracentrifuge tubes (Beckman Coulter, Brea, California, USA) and centrifuged at  $30\,000 g$  for 30 min at  $4^\circ\text{C}$  (swinging bucket SW 41 Ti Rotor, Beckman L8-70M ultracentrifuge). The pellet was collected in ice-cold HBSS, briefly sonicated and the homogenous suspension was overlaid on 8 ml of 30% Omnipaque 350 (GE Healthcare, Princeton, New Jersey, USA). After centrifugation ( $30\,000 g$ , 30 min,  $4^\circ\text{C}$ ) the floating membrane fraction (seen as a band on top of the 30% Omnipaque 350) was collected carefully, diluted 8–10 $\times$  with HBSS and sedimented ( $100\,000 g$ , 1 h,  $4^\circ\text{C}$ ). This membrane pellet was resuspended and homogenized in 2 ml of 25% OptiPrep (Sigma-Aldrich, St. Louis, Missouri, USA) in TNE buffer (20 mM Tris-HCl pH = 7.5, 150 mM NaCl, 1 mM EDTA) and placed at bottom of ultra-clear ultracentrifuge tubes to layer successively 20.0%, 17.5%, 15.0%, 12.5%, 10.0% and 0% OptiPrep in TNE. Following ultracentrifugation ( $150\,000 g$ , 16 h,  $4^\circ\text{C}$ ), membrane fractions at the 17.5%, 15.0%, 12.5% and 10.0% OptiPrep interfaces were collected, washed with 100 mM  $\text{Na}_2\text{CO}_3$  (pH = 11.5) and dissolved in 0.5% Triton X-100/TNE. Proteins in these samples were acetone precipitated and dissolved in 0.5% RapiGest SF Surfactant (Waters Corp., Milford, Maryland, USA) in 100 mM  $\text{NH}_4\text{HCO}_3$ . The pellets that were enriched in inclusion membranes (fractions 2 and 3) were analysed by the same method as above except with a single dimension of LC-MS/MS and utilizing  $1 \mu\text{g}$  extracts.

#### Protein category analysis

For comparisons between EB and RB proteomes, all proteins detected were annotated (Table S1) and grouped into functional groups and subgroups. To define the functional groups, we essentially used the classification described in the first *C. trachomatis* genome (Stephens *et al.*, 1998) and updated it based on information available in the public databases NCBI (<http://www.ncbi.nlm.nih.gov/sites/entrez>), Uniprot (<http://www.uniprot.org>), CMR (<http://cmr.jcvi.org/tigr-scripts/CMR/CMrHomePage.cgi>) and ChlamydiaeDB (<http://www.chlamydiaedb.org/portal/web/chlamydiaedb>), as well as in

specific publications when available (see Table S1). For the 'Virulence & T3S' category, we included T3S effectors (Jehl *et al.*, 2011), components and chaperones (Hefty and Stephens, 2007; Betts-Hampikian and Fields, 2010), inclusion membrane proteins (Li *et al.*, 2008a) and few other proteins originally considered as 'Pathogenesis-Associated' in previous publications [CT153 (Taylor *et al.*, 2010), SodA/CT294, PapQ/CT601, AhpC/CT603 (Stephens *et al.*, 1998)], as shown in Table S1. Most of the proteins were classified in only one functional group and a few in two or more, as indicated in Table S1. For quantitative analysis of functional categories comparing EBs and RBs, the mass corresponding to proteins within each group was summed to obtain the total mass for that group. Only proteins identified with two or more peptides were quantified and included in the category analysis. If a given protein belonged to two or more functional groups, it was counted two or more times, accordingly.

#### Protein identification numbers and proteomic data repository

Identification numbers for all 485 proteins analysed in this study as well as their corresponding primary locus in reference strain used in our experiments (*C. trachomatis* serovar L2 434/Bu) are provided in Table S1 and were retrieved from NCBI public database (<http://www.ncbi.nlm.nih.gov/protein/>). For convenience, equivalent primary loci corresponding to the widely used reference strain *C. trachomatis* serovar D UW-3/CX were also provided (Table S1) and eventually used as the primary name of the protein when no other specific name was available. The unfiltered MS data sets can be downloaded from [https://discovery.genome.duke.edu/express/resources/1635/1635\\_RB\\_exportwithMaxScores\\_042511.xlsx](https://discovery.genome.duke.edu/express/resources/1635/1635_RB_exportwithMaxScores_042511.xlsx) (for RB proteome) and [https://discovery.genome.duke.edu/express/resources/1635/1635\\_EB\\_exportwithMaxScores\\_042511.xlsx](https://discovery.genome.duke.edu/express/resources/1635/1635_EB_exportwithMaxScores_042511.xlsx) (for EB proteome).

#### Acknowledgements

We thank K. Fields and M. Horn for comments and feedback on this manuscript, A. Xavier, M. Tan, K. Fields, H. Caldwell and T. Hackstadt for reagents. Special thanks to Dr Keith Fadgen and Dr Martha Stapels of Waters Corporation for technical assistance and method development with the 2DLC, and to Waters Corporation for providing the 2D nanoAcquity. This work was supported by grants from the NIH (AI096320 and 1AI068032-04S1) and the Burroughs Wellcome Trust Program in Infectious Diseases. The Duke Proteomics Core Facility is supported in part by Duke University's CTSA Grant 10 L1 RR024128-01 from NCRR/NIH. H.A. Saka was supported by a fellowship from the Pew Latin American Fellows Program in the Biomedical Sciences.

#### References

- Albrecht, M., Sharma, C.M., Reinhardt, R., Vogel, J., and Rudel, T. (2010) Deep sequencing-based discovery of the *Chlamydia trachomatis* transcriptome. *Nucleic Acids Res* **38**: 868–877.
- Bannantine, J.P., Griffiths, R.S., Viratyosin, W., Brown, W.J., and Rockey, D.D. (2000) A secondary structure motif predictive of protein localization to the chlamydial inclusion membrane. *Cell Microbiol* **2**: 35–47.
- Bebear, C., and de Barbeyrac, B. (2009) Genital *Chlamydia trachomatis* infections. *Clin Microbiol Infect* **15**: 4–10.
- Beeckman, D.S., and Vanrompay, D.C. (2010) Bacterial secretion systems with an emphasis on the chlamydial Type III secretion system. *Curr Issues Mol Biol* **12**: 17–41.
- Belland, R.J., Zhong, G., Crane, D.D., Hogan, D., Sturdevant, D., Sharma, J., *et al.* (2003) Genomic transcriptional profiling of the developmental cycle of *Chlamydia trachomatis*. *Proc Natl Acad Sci USA* **100**: 8478–8483.
- Betts, H.J., Wolf, K., and Fields, K.A. (2009) Effector protein modulation of host cells: examples in the *Chlamydia* spp. arsenal. *Curr Opin Microbiol* **12**: 81–87.
- Betts-Hampikian, H.J., and Fields, K.A. (2010) The chlamydial type III secretion mechanism: revealing cracks in a tough nut. *Front Microbiol* **1**: 1–13.
- Bhavsar, A.P., Auweter, S.D., and Finlay, B.B. (2010) Proteomics as a probe of microbial pathogenesis and its molecular boundaries. *Future Microbiol* **5**: 253–265.
- Birkelund, S., Morgan-Fisher, M., Timmerman, E., Gevaert, K., Shaw, A.C., and Christiansen, G. (2009) Analysis of proteins in *Chlamydia trachomatis* L2 outer membrane complex, COMC. *FEMS Immunol Med Microbiol* **55**: 187–195.
- Bradford, M.M. (1976) A rapid and sensitive method for the quantitation of microgram quantities of protein utilizing the principle of protein-dye binding. *Anal Biochem* **72**: 248–254.
- Burton, M.J., and Mabey, D.C. (2009) The global burden of trachoma: a review. *PLoS Negl Trop Dis* **3**: e460.
- Caldwell, H.D., Kromhout, J., and Schachter, J. (1981) Purification and partial characterization of the major outer membrane protein of *Chlamydia trachomatis*. *Infect Immun* **31**: 1161–1176.
- Clifton, D.R., Fields, K.A., Grieshaber, S.S., Dooley, C.A., Fischer, E.R., Mead, D.J., *et al.* (2004) A chlamydial type III translocated protein is tyrosine-phosphorylated at the site of entry and associated with recruitment of actin. *Proc Natl Acad Sci USA* **101**: 10166–10171.
- Cocchiaro, J.L., Kumar, Y., Fischer, E.R., Hackstadt, T., and Valdivia, R.H. (2008) Cytoplasmic lipid droplets are translocated into the lumen of the *Chlamydia trachomatis* parasitophorous vacuole. *Proc Natl Acad Sci USA* **105**: 9379–9384.
- Crane, D.D., Carlson, J.H., Fischer, E.R., Bavoil, P., Hsia, R.C., Tan, C., *et al.* (2006) *Chlamydia trachomatis* polymorphic membrane protein D is a species-common pan-neutralizing antigen. *Proc Natl Acad Sci USA* **103**: 1894–1899.
- Darville, T. (2005) *Chlamydia trachomatis* infections in neonates and young children. *Semin Pediatr Infect Dis* **16**: 235–244.
- Dautry-Varsat, A., Subtil, A., and Hackstadt, T. (2005) Recent insights into the mechanisms of *Chlamydia* entry. *Cell Microbiol* **7**: 1714–1722.
- Dean, D. (2006) Lessons and challenges arising from the 'first wave' of *Chlamydia* genome sequencing. In *Chlamydia Genomics and Pathogenesis*. Bavoil, P.M., and Wyrick, P.B. (eds). Wymondham, Norfolk, UK: Horizon Bioscience, pp. 1–25.



- Delahunty, C., and Yates, J.R., 3rd (2005) Protein identification using 2D-LC-MS/MS. *Methods* **35**: 248–255.
- Dowell, J.A., Frost, D.C., Zhang, J., and Li, L. (2008) Comparison of two-dimensional fractionation techniques for shotgun proteomics. *Anal Chem* **80**: 6715–6723.
- Erhardt, M., and Hughes, K.T. (2010) C-ring requirement in flagellar type III secretion is bypassed by FliDC upregulation. *Mol Microbiol* **75**: 376–393.
- Forgacs, M. (2007) Vacuolar ATPases: rotary proton pumps in physiology and pathophysiology. *Nat Rev Mol Cell Biol* **8**: 917–929.
- Galan, J.E., and Wolf-Watz, H. (2006) Protein delivery into eukaryotic cells by type III secretion machines. *Nature* **444**: 567–573.
- Geromanos, S.J., Vissers, J.P., Silva, J.C., Dorschel, C.A., Li, G.Z., Gorenstein, M.V., *et al.* (2009) The detection, correlation, and comparison of peptide precursor and product ions from data independent LC-MS with data dependant LC-MS/MS. *Proteomics* **9**: 1683–1695.
- Gilar, M., Olivova, P., Daly, A.E., and Gebler, J.C. (2005a) Orthogonality of separation in two-dimensional liquid chromatography. *Anal Chem* **77**: 6426–6434.
- Gilar, M., Olivova, P., Daly, A.E., and Gebler, J.C. (2005b) Two-dimensional separation of peptides using RP-RP-HPLC system with different pH in first and second separation dimensions. *J Sep Sci* **28**: 1694–1703.
- Giles, D.K., Whittimore, J.D., LaRue, R.W., Raulston, J.E., and Wyrick, P.B. (2006) Ultrastructural analysis of chlamydial antigen-containing vesicles everting from the *Chlamydia trachomatis* inclusion. *Microbes Infect* **8**: 1579–1591.
- Gomes, J.P., Nunes, A., Bruno, W.J., Borrego, M.J., Florindo, C., and Dean, D. (2006) Polymorphisms in the nine polymorphic membrane proteins of *Chlamydia trachomatis* across all serovars: evidence for serovar Da recombination and correlation with tissue tropism. *J Bacteriol* **188**: 275–286.
- Gonzalez-Pedrajo, B., Minamino, T., Kihara, M., and Namba, K. (2006) Interactions between C ring proteins and export apparatus components: a possible mechanism for facilitating type III protein export. *Mol Microbiol* **60**: 984–998.
- Grimwood, J., Olinger, L., and Stephens, R.S. (2001) Expression of *Chlamydia pneumoniae* polymorphic membrane protein family genes. *Infect Immun* **69**: 2383–2389.
- Haggerty, C.L., Gottlieb, S.L., Taylor, B.D., Low, N., Xu, F., and Ness, R.B. (2010) Risk of sequelae after *Chlamydia trachomatis* genital infection in women. *J Infect Dis* **201** (Suppl. 2): S134–S155.
- Hatch, T.P., Allan, I., and Pearce, J.H. (1984) Structural and polypeptide differences between envelopes of infective and reproductive life cycle forms of *Chlamydia* spp. *J Bacteriol* **157**: 13–20.
- Hefty, P.S., and Stephens, R.S. (2007) Chlamydial type III secretion system is encoded on ten operons preceded by sigma 70-like promoter elements. *J Bacteriol* **189**: 198–206.
- Henderson, I.R., Navarro-Garcia, F., Desvaux, M., Fernandez, R.C., and Ala'Aldeen, D. (2004) Type V protein secretion pathway: the autotransporter story. *Microbiol Mol Biol Rev* **68**: 692–744.
- Howie, S.E., Horner, P.J., Horne, A.W., and Entrican, G. (2011) Immunity and vaccines against sexually transmitted *Chlamydia trachomatis* infection. *Curr Opin Infect Dis* **24**: 56–61.
- Hybiske, K., and Stephens, R.S. (2007) Mechanisms of host cell exit by the intracellular bacterium *Chlamydia*. *Proc Natl Acad Sci USA* **104**: 11430–11435.
- Jehl, M.A., Arnold, R., and Rattei, T. (2011) Effective – a database of predicted secreted bacterial proteins. *Nucleic Acids Res* **39**: D591–D595.
- Jewett, T.J., Miller, N.J., Dooley, C.A., and Hackstadt, T. (2010) The conserved Tarp actin binding domain is important for chlamydial invasion. *PLoS Pathog* **6**: e1000997.
- Johnson, D.L., Stone, C.B., and Mahony, J.B. (2008) Interactions between CdsD, CdsQ, and CdsL, three putative *Chlamydia pneumoniae* type III secretion proteins. *J Bacteriol* **190**: 2972–2980.
- Jouihri, N., Sory, M.P., Page, A.L., Gounon, P., Parsot, C., and Allaoui, A. (2003) MxiK and MxiN interact with the Spa47 ATPase and are required for transit of the needle components MxiH and MxiI, but not of Ipa proteins, through the type III secretion apparatus of *Shigella flexneri*. *Mol Microbiol* **49**: 755–767.
- Keller, A., Nesvizhskii, A.I., Kolker, E., and Aebersold, R. (2002) Empirical statistical model to estimate the accuracy of peptide identifications made by MS/MS and database search. *Anal Chem* **74**: 5383–5392.
- Kiselev, A.O., Stamm, W.E., Yates, J.R., and Lampe, M.F. (2007) Expression, processing, and localization of PmpD of *Chlamydia trachomatis* Serovar L2 during the chlamydial developmental cycle. *PLoS ONE* **2**: e568.
- Kiselev, A.O., Skinner, M.C., and Lampe, M.F. (2009) Analysis of pmpD expression and PmpD post-translational processing during the life cycle of *Chlamydia trachomatis* serovars A, D, and L2. *PLoS ONE* **4**: e5191.
- Koehler, J.E., Birkelund, S., and Stephens, R.S. (1992) Overexpression and surface localization of the *Chlamydia trachomatis* major outer membrane protein in *Escherichia coli*. *Mol Microbiol* **6**: 1087–1094.
- Konishi, M., Kanbe, M., McMurry, J.L., and Aizawa, S. (2009) Flagellar formation in C-ring-defective mutants by overproduction of FliI, the ATPase specific for flagellar type III secretion. *J Bacteriol* **191**: 6186–6191.
- van Kuppeveld, F.J., van der Logt, J.T., Angulo, A.F., van Zoest, M.J., Quint, W.G., Niesters, H.G., *et al.* (1992) Genus- and species-specific identification of mycoplasmas by 16S rRNA amplification. *Appl Environ Microbiol* **58**: 2606–2615.
- Li, G.Z., Vissers, J.P., Silva, J.C., Golick, D., Gorenstein, M.V., and Geromanos, S.J. (2009) Database searching and accounting of multiplexed precursor and product ion spectra from the data independent analysis of simple and complex peptide mixtures. *Proteomics* **9**: 1696–1719.
- Li, Z., Chen, C., Chen, D., Wu, Y., Zhong, Y., and Zhong, G. (2008a) Characterization of fifty putative inclusion membrane proteins encoded in the *Chlamydia trachomatis* genome. *Infect Immun* **76**: 2746–2757.
- Li, Z., Chen, D., Zhong, Y., Wang, S., and Zhong, G. (2008b) The chlamydial plasmid-encoded protein pgp3 is secreted into the cytosol of *Chlamydia*-infected cells. *Infect Immun* **76**: 3415–3428.
- Liu, X., Afrane, M., Clemmer, D.E., Zhong, G., and Nelson, D.E. (2010) Identification of *Chlamydia trachomatis* outer

- membrane complex proteins by differential proteomics. *J Bacteriol* **192**: 2852–2860.
- Longbottom, D., Russell, M., Dunbar, S.M., Jones, G.E., and Herring, A.J. (1998) Molecular cloning and characterization of the genes coding for the highly immunogenic cluster of 90-kilodalton envelope proteins from the *Chlamydia psittaci* subtype that causes abortion in sheep. *Infect Immun* **66**: 1317–1324.
- McClarty, G. (1999) Chlamydial metabolism as inferred from the complete genome sequence. In *Chlamydia: Intracellular Biology, Pathogenesis and Immunity*. Stephens, R.S. (ed.). Washington, DC: American Society for Microbiology, pp. 69–98.
- Markham, A.P., Jaafar, Z.A., Kemege, K.E., Middaugh, C.R., and Hefty, P.S. (2009) Biophysical characterization of *Chlamydia trachomatis* CT584 supports its potential role as a type III secretion needle tip protein. *Biochemistry* **48**: 10353–10361.
- Meng, F., Wiener, M.C., Sachs, J.R., Burns, C., Verma, P., Paweletz, C.P., et al. (2007) Quantitative analysis of complex peptide mixtures using FTMS and differential mass spectrometry. *J Am Soc Mass Spectrom* **18**: 226–233.
- Miller, J.D., Sal, M.S., Schell, M., Whittimore, J.D., and Raulston, J.E. (2009) *Chlamydia trachomatis* YtgA is an iron-binding periplasmic protein induced by iron restriction. *Microbiology* **155**: 2884–2894.
- Miller, W.C., Ford, C.A., Morris, M., Handcock, M.S., Schmitz, J.L., Hobbs, M.M., et al. (2004) Prevalence of chlamydial and gonococcal infections among young adults in the United States. *JAMA* **291**: 2229–2236.
- Moorhead, A.M., Jung, J.Y., Smirnov, A., Kaufer, S., and Scidmore, M.A. (2010) Multiple host proteins that function in phosphatidylinositol-4-phosphate metabolism are recruited to the chlamydial inclusion. *Infect Immun* **78**: 1990–2007.
- Morita-Ishihara, T., Ogawa, M., Sagara, H., Yoshida, M., Katayama, E., and Sasakawa, C. (2006) Shigella Spa33 is an essential C-ring component of type III secretion machinery. *J Biol Chem* **281**: 599–607.
- Mukhopadhyay, S., Miller, R.D., and Summersgill, J.T. (2004) Analysis of altered protein expression patterns of *Chlamydia pneumoniae* by an integrated proteome-works system. *J Proteome Res* **3**: 878–883.
- Nesvizhskii, A.I., Keller, A., Kolker, E., and Aebersold, R. (2003) A statistical model for identifying proteins by tandem mass spectrometry. *Anal Chem* **75**: 4646–4658.
- Nicholson, T.L., Olinger, L., Chong, K., Schoolnik, G., and Stephens, R.S. (2003) Global stage-specific gene regulation during the developmental cycle of *Chlamydia trachomatis*. *J Bacteriol* **185**: 3179–3189.
- Nilsson, T., Mann, M., Aebersold, R., Yates, J.R., 3rd, Bairoch, A., and Bergeron, J.J. (2010) Mass spectrometry in high-throughput proteomics: ready for the big time. *Nat Methods* **7**: 681–685.
- Numoto, N., Hasegawa, Y., Takeda, K., and Miki, K. (2009) Inter-subunit interaction and quaternary rearrangement defined by the central stalk of prokaryotic V1-ATPase. *EMBO Rep* **10**: 1228–1234.
- O'Connell, C.M., and Nicks, K.M. (2006) A plasmid-cured *Chlamydia muridarum* strain displays altered plaque morphology and reduced infectivity in cell culture. *Microbiology* **152**: 1601–1607.
- Paweletz, C.P., Wiener, M.C., Bondarenko, A.Y., Yates, N.A., Song, Q., Liaw, A., et al. (2010) Application of an end-to-end biomarker discovery platform to identify target engagement markers in cerebrospinal fluid by high resolution differential mass spectrometry. *J Proteome Res* **9**: 1392–1401.
- Peters, J., Wilson, D.P., Myers, G., Timms, P., and Bavoil, P.M. (2007) Type III secretion in *Chlamydia*. *Trends Microbiol* **15**: 241–251.
- Peterson, E.M., Cheng, X., Markoff, B.A., Fielder, T.J., and de la Maza, L.M. (1991) Functional and structural mapping of *Chlamydia trachomatis* species-specific major outer membrane protein epitopes by use of neutralizing monoclonal antibodies. *Infect Immun* **59**: 4147–4153.
- Phillips, D.M., Swenson, C.E., and Schachter, J. (1984) Ultrastructure of *Chlamydia trachomatis* infection of the mouse oviduct. *J Ultrastruct Res* **88**: 244–256.
- Raulston, J.E., Miller, J.D., Davis, C.H., Schell, M., Baldwin, A., Ferguson, K., and Lane, H. (2007) Identification of an iron-responsive protein that is antigenic in patients with *Chlamydia trachomatis* genital infections. *FEMS Immunol Med Microbiol* **51**: 569–576.
- Read, T.D., Brunham, R.C., Shen, C., Gill, S.R., Heidelberg, J.F., White, O., et al. (2000) Genome sequences of *Chlamydia trachomatis* MoPn and *Chlamydia pneumoniae* AR39. *Nucleic Acids Res* **28**: 1397–1406.
- Read, T.D., Myers, G.S., Brunham, R.C., Nelson, W.C., Paulsen, I.T., Heidelberg, J., et al. (2003) Genome sequence of *Chlamydophila caviae* (*Chlamydia psittaci* GPIC): examining the role of niche-specific genes in the evolution of the Chlamydiaceae. *Nucleic Acids Res* **31**: 2134–2147.
- Reidel, B., Thompson, J.W., Farsiu, S., Moseley, M.A., Skiba, N.P., and Arshavsky, V.Y. (2011) Proteomic profiling of a layered tissue reveals unique glycolytic specializations of photoreceptor cells. *Mol Cell Proteomics* **10**: M110.002469, doi:10.1074/mcp.M110.002469.
- Saka, H.A., and Valdivia, R.H. (2010) Acquisition of nutrients by Chlamydiae: unique challenges of living in an intracellular compartment. *Curr Opin Microbiol* **13**: 4–10.
- Scidmore-Carlson, M.A., Shaw, E.I., Dooley, C.A., Fischer, E.R., and Hackstadt, T. (1999) Identification and characterization of a *Chlamydia trachomatis* early operon encoding four novel inclusion membrane proteins. *Mol Microbiol* **33**: 753–765.
- Shaw, A.C., Gevaert, K., Demol, H., Hoorelbeke, B., Vandekerckhove, J., Larsen, M.R., et al. (2002) Comparative proteome analysis of *Chlamydia trachomatis* serovar A, D and L2. *Proteomics* **2**: 164–186.
- Silva, J.C., Denny, R., Dorschel, C., Gorenstein, M.V., Li, G.Z., Richardson, K., et al. (2006a) Simultaneous qualitative and quantitative analysis of the *Escherichia coli* proteome: a sweet tale. *Mol Cell Proteomics* **5**: 589–607.
- Silva, J.C., Gorenstein, M.V., Li, G.Z., Vissers, J.P., and Geronimos, S.J. (2006b) Absolute quantification of proteins by LCMSE: a virtue of parallel MS acquisition. *Mol Cell Proteomics* **5**: 144–156.
- Sixt, B.S., Heinz, C., Pichler, P., Heinz, E., Montanaro, J., Op den Camp, H.J., et al. (2011) Proteomic analysis reveals a virtually complete set of proteins for translation and energy

- generation in elementary bodies of the amoeba symbiont *Protochlamydia amoebophila*. *Proteomics* **11**: 1868–1892.
- Skipp, P., Robinson, J., O'Connor, C.D., and Clarke, I.N. (2005) Shotgun proteomic analysis of *Chlamydia trachomatis*. *Proteomics* **5**: 1558–1573.
- Spaeth, K.E., Chen, Y.S., and Valdivia, R.H. (2009) The *Chlamydia* type III secretion system C-ring engages a chaperone–effector protein complex. *PLoS Pathog* **5**: e1000579.
- Stamm, W.E. (1999) *Chlamydia trachomatis* infections: progress and problems. *J Infect Dis* **179** (Suppl. 2): S380–S383.
- Stephens, R.S., Kalman, S., Lammel, C., Fan, J., Marathe, R., Aravind, L., *et al.* (1998) Genome sequence of an obligate intracellular pathogen of humans: *Chlamydia trachomatis*. *Science* **282**: 754–759.
- Stone, C.B., Johnson, D.L., Bulir, D.C., Gilchrist, J.D., and Mahony, J.B. (2008) Characterization of the putative type III secretion ATPase CdsN (Cpn0707) of *Chlamydomphila pneumoniae*. *J Bacteriol* **190**: 6580–6588.
- Tan, C., Hsia, R.C., Shou, H., Carrasco, J.A., Rank, R.G., and Bavoil, P.M. (2010) Variable expression of surface-exposed polymorphic membrane proteins in *in vitro*-grown *Chlamydia trachomatis*. *Cell Microbiol* **12**: 174–187.
- Tanzer, R.J., and Hatch, T.P. (2001) Characterization of outer membrane proteins in *Chlamydia trachomatis* LGV serovar L2. *J Bacteriol* **183**: 2686–2690.
- Taylor, L.D., Nelson, D.E., Dorward, D.W., Whitmire, W.M., and Caldwell, H.D. (2010) Biological characterization of *Chlamydia trachomatis* plasticity zone MACPF domain family protein CT153. *Infect Immun* **78**: 2691–2699.
- Thomas, J.A., Weintraub, S.T., Hakala, K., Serwer, P., and Hardies, S.C. (2010) Proteome of the large *Pseudomonas myovirus* 201 phi 2-1: delineation of proteolytically processed virion proteins. *Mol Cell Proteomics* **9**: 940–951.
- Thomson, N.R., Holden, M.T., Carder, C., Lennard, N., Lockey, S.J., Marsh, P., *et al.* (2008) *Chlamydia trachomatis*: genome sequence analysis of lymphogranuloma venereum isolates. *Genome Res* **18**: 161–171.
- Tipples, G., and McClarty, G. (1993) The obligate intracellular bacterium *Chlamydia trachomatis* is auxotrophic for three of the four ribonucleoside triphosphates. *Mol Microbiol* **8**: 1105–1114.
- Tjaden, J., Winkler, H.H., Schwoppe, C., Van Der Laan, M., Mohlmann, T., and Neuhaus, H.E. (1999) Two nucleotide transport proteins in *Chlamydia trachomatis*, one for net nucleoside triphosphate uptake and the other for transport of energy. *J Bacteriol* **181**: 1196–1202.
- Valdivia, R.H. (2008) *Chlamydia* effector proteins and new insights into chlamydial cellular microbiology. *Curr Opin Microbiol* **11**: 53–59.
- Vandahl, B.B., Birkelund, S., Demol, H., Hoorelbeke, B., Christiansen, G., Vandekerckhove, J., and Gevaert, K. (2001) Proteome analysis of the *Chlamydia pneumoniae* elementary body. *Electrophoresis* **22**: 1204–1223.
- Vandahl, B.B., Birkelund, S., and Christiansen, G. (2002a) Proteome analysis of *Chlamydia pneumoniae*. *Methods Enzymol* **358**: 277–288.
- Vandahl, B.B., Pedersen, A.S., Gevaert, K., Holm, A., Vandekerckhove, J., Christiansen, G., and Birkelund, S. (2002b) The expression, processing and localization of polymorphic membrane proteins in *Chlamydia pneumoniae* strain CWL029. *BMC Microbiol* **2**: 36.
- Wagar, E.A., and Stephens, R.S. (1988) Developmental-form-specific DNA-binding proteins in *Chlamydia* spp. *Infect Immun* **56**: 1678–1684.
- Walther, T.C., and Mann, M. (2010) Mass spectrometry-based proteomics in cell biology. *J Cell Biol* **190**: 491–500.
- Watson, M.W., Lambden, P.R., Everson, J.S., and Clarke, I.N. (1994) Immunoreactivity of the 60 kDa cysteine-rich proteins of *Chlamydia trachomatis*, *Chlamydia psittaci* and *Chlamydia pneumoniae* expressed in *Escherichia coli*. *Microbiology* **140** (Part 8): 2003–2011.
- Wehrl, W., Meyer, T.F., Jungblut, P.R., Muller, E.C., and Szczepek, A.J. (2004) Action and reaction: *Chlamydomphila pneumoniae* proteome alteration in a persistent infection induced by iron deficiency. *Proteomics* **4**: 2969–2981.
- WHO (2001) Global prevalence and incidence of selected curable sexually transmitted infections: overview and estimates [WWW document]. URL: [http://www.who.int/hiv/pub/sti/who\\_hiv\\_aids\\_2001.02.pdf](http://www.who.int/hiv/pub/sti/who_hiv_aids_2001.02.pdf) (accessed 6 August 2010).
- WHO (2003) Report of the 2nd global scientific meeting on trachoma WHO/PBD/GET 03.1 [WWW document]. URL: <http://www.who.int/blindness/2nd%20GLOBAL%20SCIENTIFIC%20MEETING.pdf> (accessed 6 August 2010).
- Yip, C.K., Finlay, B.B., and Strynadka, N.C. (2005) Structural characterization of a type III secretion system filament protein in complex with its chaperone. *Nat Struct Mol Biol* **12**: 75–81.
- Zhang, Y.X., Stewart, S., Joseph, T., Taylor, H.R., and Caldwell, H.D. (1987) Protective monoclonal antibodies recognize epitopes located on the major outer membrane protein of *Chlamydia trachomatis*. *J Immunol* **138**: 575–581.

## Supporting information

Additional supporting information may be found in the online version of this article.

Please note: Wiley-Blackwell are not responsible for the content or functionality of any supporting materials supplied by the authors. Any queries (other than missing material) should be directed to the corresponding author for the article.